Electronic Supplementary Material (ESI) for ChemComm.

Porous Organic Crystals Crosslinked by Free-radical Reactions

Krishanu Samanta,[1] Jiashan Mi,[2, 3] Albert D. Chen,[1] Fangzhou Li,[4] Richard J. Staples,[5] Aaron J. Rossini,[2, 3] Chenfeng Ke[1, 4,*]

[1] *Department of Chemistry, Dartmouth College, 41 College Street, Hanover, NH 03755, USA*
[2] *Department of Chemistry, Iowa State University, 2438 Pammel Drive, Ames, IA 50011, USA*
[3] *US DOE Ames National Laboratory, Ames, Iowa, USA, 50011*
[4] *Department of Chemistry, Washington University in St. Louis, One Brookings Drive, St. Louis, MO 63130, USA*
[5] *Department of Chemistry, Michigan State University, 578 S. Shaw Lane, East Lansing, MI 48824, USA*
Email: cke@wustl.edu

Table of Contents

S1. General Information.

All the reagents and solvents were purchased from commercial sources, like Fisher Scientific, Sigma-Aldrich, and VWR, and used as it is without further purification.

^{1}H and ^{13}C NMR spectra were recorded on either a Bruker AVIII 500 or Bruker AVIII 600 MHz Spectrometer and the peaks were assigned using residual solvent peak as the reference. The working frequency for ^{13}C is 150 MHz.

Solid-state NMR experiments were recorded at B_0 = 9.4 T [$\nu_0(^{1}H)$ = 400.5 MHz, $\nu_0(^{11}B)$ = 80.1 MHz, $\nu_0(^{13}C)$ = 100.7 MHz] Bruker Avance III HD spectrometer with a wide-bore magnet. A Bruker 2.5 mm magic angle spinning (MAS) HXY NMR probe configured in double-resonance mode was used to perform all fast-MAS experiments at a spinning rate (ν_{rot}) of 25 kHz. All samples were packed into the zirconia 2.5 mm NMR rotor on a benchtop, and the NMR rotors were spun with N_2 gas. Chemical shifts were calibrated by using neat tetramethylsilane (TMS) with adamantane as a secondary chemical shift reference ($\delta(^{1}H)$ = 1.71 ppm). ^{11}B and ^{13}C shifts were indirectly referenced by using previously reported IUPAC recommended relative NMR frequencies.[1] All spectra were processed with the Bruker Topspin 3.6.4 NMR software. All experimental NMR parameters (MAS, number of scans, recycle delays (the optimum recycle delays of 1.3 × T_1 to maximize sensitivity), CP/recoupling duration, and total experimental times) of all experiments are listed in Table S4. All ^{1}H $\pi/2$ and π pulse lengths were 2.5 and 5 μs in duration, corresponding to a 100 kHz radio frequency (RF) field. ^{13}C solid-state NMR spectra were acquired with cross-polarization for signal enhancement.[2] ^{1}H-^{13}C cross-polarization (CP) matching conditions were optimized on an external standard of adamantane. All ^{1}H CP spin-lock RF fields were linearly ramped from 90% to 100% amplitude[3] to broaden the Hartman−Hahn match condition. The ^{1}H–^{13}C CP experiments used spin lock pulses with RF fields of ca. 93 kHz and 66 kHz for ^{1}H and ^{13}C, respectively. SPINAL-64 heteronuclear decoupling[4] with a ^{1}H RF field of 100 kHz was applied during the acquisition.

High-resolution mass spectrometry (HRMS) data was collected on a Synapt G2-Si mass spectrometer by the Mass Spectrometry Laboratory at the University of Illinois, Urbana-Champaign. The elemental analysis was carried out by Intertek Pharmaceutical Services (Whitehouse, NJ).

Fourier transform infrared (FT-IR) spectra were collected on a Jasco 6200 spectrometer. Powder X-ray Diffraction (PXRD) patterns were obtained from a Rigaku MiniFlex powder X-ray diffractometer, and single crystal diffraction (SCXRD) data were collected on a Rigaku Synergy S single crystal diffractometer. Thermogravimetric analysis (TGA) was performed on a TA instrument discovery 55 thermal gravimetric analyzer. The samples were placed on a platinum pan kept under a nitrogen atmosphere and the data was collected from room temperature to 900 °C with a ramp rate of 10 °C/min. Optical microscope images were captured using a NIKON SMZ-2T stereomicroscope.

For the gas sorption and solvent vapor sorption analysis, all the samples were activated using supercritical CO_2 using a Samdri 795 Critical Point Drye and then kept under a dynamic vacuum for 24 h at 80 °C to degas the samples. The sorption analyses were performed on a Micromeritics FLEX 3.0 surface area analyzer. The CO_2 sorption isotherm was measured using an ice bath at 273 K or dry-ice acetone at 195 K and the N_2 sorption was carried out at 77 K using a liquid nitrogen bath. All solvent vapor sorption analyses were conducted at 296 K, keeping the solvent chamber at 40 °C (30 °C in the case of pentane).

S2. Synthesis and Characterizations of monomers

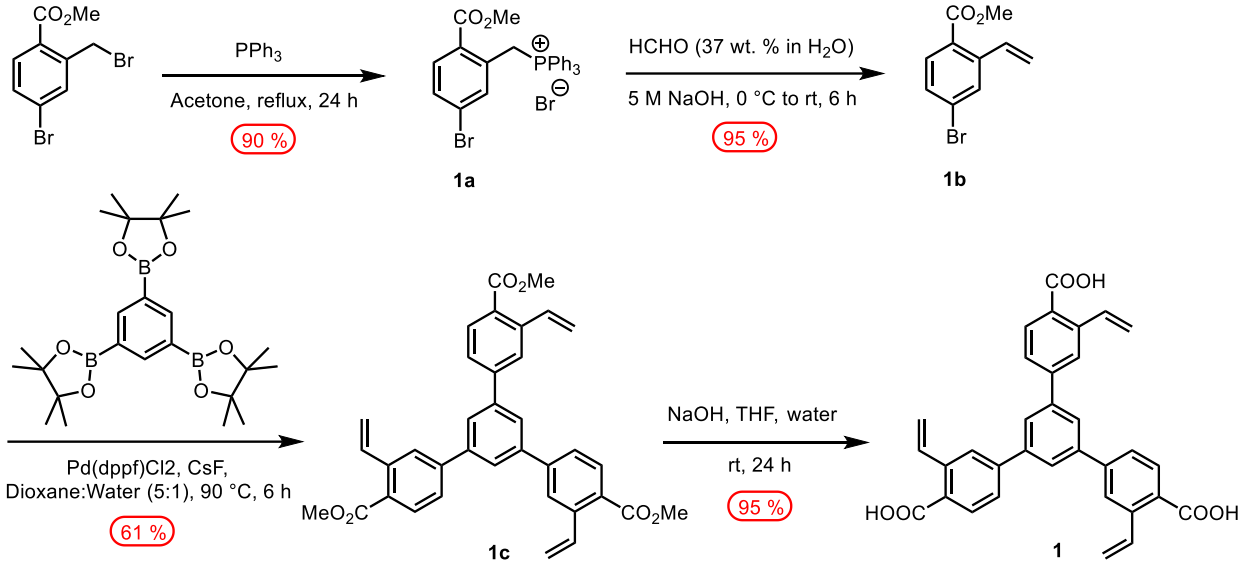

Scheme S1. Synthesis of monomer **1**

1a. Compound **1a** was synthesized according to a previously reported method.[5] Methyl 4-bromo-2-bromomethylbenzoate (10.0 g, 32.47 mmol, 1.0 *equiv*.) and triphenylphosphine (10.22 g, 38.96 mmol, 1.2 *equiv*.) were dissolved in acetone (100 mL). The reaction mixture was refluxed for 24 hours and then cooled to room temperature. After that, the resulting white precipitate was filtered and washed with acetone (20 mL × 3) to obtain compound **1a** as a white powder (16.66 g, 29.22 mmol) in 90 % yield.
^{1}H NMR (500 MHz, DMSO-d_6, 298 K): δ = 7.92 (t, *J* = 7.6 Hz, 3H), 7.75 (td, *J* = 7.9, 3.8 Hz, 8H), 7.61 (dd, *J* = 12.8, 7.8 Hz, 6H), 7.53 (s, 1H), 5.56 (d, *J* = 15.6 Hz, 2H), 3.44 (s, 3H).

1b. Compound **1b** was synthesized following a previously reported method.[1] Formaldehyde solution (30 mL, 37 wt. % in water) was added to **S1a** (5.5 g, 9.64 mmol), and the mixture was cooled to 0 °C. To it, 5 M NaOH aqueous solution (12 mL) was added dropwise over a half-hour period. The reaction was then allowed to warm to room temperature and further stirred for 6 h. After that, water (50 mL) and chloroform (150 mL) were added to the reaction mixture. The organic layer was separated and dried over anhydrous Na_2SO_4 and then removed under a vacuum. The crude product was subjected to silica gel chromatography with n-hexane/CH_2Cl_2 (9/1, v/v) as the eluent to yield compound **1b** as a colorless liquid (2.2 g, 9.16 mmol) in 95 % yield.
^{1}H NMR (500 MHz, $CDCl_3$, 298 K) δ = 7.76 (d, *J* = 8.4 Hz, 1H), 7.72 (d, *J* = 2.0 Hz, 1H), 7.47 – 7.39 (m, 2H), 5.66 (dd, *J* = 17.4, 1.1 Hz, 1H), 5.40 (dd, *J* = 10.9, 1.1 Hz, 1H), 3.89 (s, 3H).

1c. 1,3,5-Phenyltriboronic acid tris(pinacol) ester (1.0 g, 2.19 mmol, 1.0 *equiv*.), **1b** (1.85 g, 7.67 mmol, 3.5 *equiv*.), CsF (2.0 g, 13.15 mmol, 6.0 *equiv*.) and Pd(dppf)Cl_2. (0.107 g, 0.13 mmol, 0.06 eq) were mixed in a mixture of 1,4-dioxane (50 mL) and water (10 mL). The flask was cooled to –78 °C and subjected to three freeze-pump-thaw cycles under the N_2 atmosphere. After the reaction was warmed to room temperature, it was stirred and heated at 90 °C for 24 h under an N_2 atmosphere. Thereafter, the reaction was cooled to room temperature, and deionized water (250 mL) was added to the reaction mixture. The solution was extracted with CH_2Cl_2 (50 mL × 3). The combined organic layer was dried over anhydrous sodium sulfate and the solvent was removed under vacuum. The crude product was subjected to silica gel chromatography with CH_2Cl_2/n-hexane (4/1, v/v) as the eluent to yield compound **1c** as a white powder (0.75 g, 1.34 mmol) in 61 % yield.

^{1}H NMR (500 MHz, $CDCl_3$, 298 K) δ = 8.04 (d, *J* = 8.1 Hz, 1H), 7.85 (s, 2H), 7.64 (dd, *J* = 8.1, 1.9 Hz, 1H), 7.57 (dd, *J* = 17.4, 11.0 Hz, 1H), 5.75 (dd, *J* = 17.4, 1.2 Hz, 1H), 5.43 (dd, *J* = 11.0, 1.2 Hz, 1H), 3.95 (s, 3H).
^{13}C NMR (150 MHz, $CDCl_3$, 298 K) δ = 167.54, 144.36, 141.69, 140.53, 135.96, 131.25, 127.73, 126.36, 126.31, 126.09, 117.10, 52.23.

Monomer 1. **1c** (0.75 g, 1.34 mmol, 1 *equiv*.) was dissolved in a mixed solution of THF (30 mL) and 1.0 M aqueous NaOH (14 mL, 14.0 mmol, 10 *equiv*.). The reaction was stirred at room temperature for 24 h. Then, the THF was removed under reduced pressure and concentrated aqueous HCl (12 M) was added to the reaction mixture until the pH of the solution reached 1.0. The generated white precipitate was collected by filtration, washed with an excess of water, and then further washed with CH_2Cl_2. The product was air-dried to afford **S1** as a white powder (0.60 g, 1.16 mmol, yield 98 %).
^{1}H NMR (500 MHz, DMSO-d_6, 298 K) δ = 13.10 (s, 1H), 8.11 (d, *J* = 2.2 Hz, 2H), 8.02 – 7.84 (m, 2H), 7.53 (dd, *J* = 17.5, 11.1 Hz, 1H), 6.01 (d, *J* = 17.1 Hz, 1H), 5.42 (d, *J* = 11.2 Hz, 1H).
^{13}C NMR (150 MHz, DMSO-d_6, 298 K) δ = 168.40, 143.21, 140.82, 138.87, 135.14, 130.81, 128.75, 126.71, 125.87, 125.45, 117.45.
HR-ESI-MS: calcd. for $C_{33}H_{24}O_6$ $[M + H]^+$ m/z = 517.1651, found m/z = 517.1646.

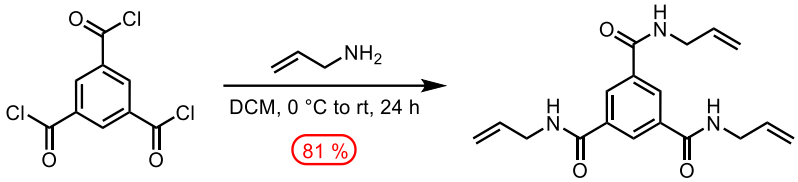

Scheme S2. Synthesis of triallyl benzamide (TAB)

TAB. Allylamine (10.7 g, 188 mmol, 5 *equiv*.) was dissolved in anhydrous CH_2Cl_2 (50 mL) and the solution was cooled to 0 °C. To it, 1,3,5-benzenetricarbonyl trichloride (10.0 g, 37.6 mmol, 1.0 *equiv*.) in CH_2Cl_2 (10 mL) was added dropwise under stirring conditions. Then, the reaction mixture was stirred at room temperature for 24 h. Then, the CH_2Cl_2 was removed under reduced pressure and the crude product was washed with 0.5 N HCl (100 mL) followed by washing with saturated sodium bicarbonate solution (100 mL). Finally, the product was washed with water and air-dried to afford TAB as a white powder (10 g, 30.5 mmol, yield 81 %).
^{1}H NMR (500 MHz, DMSO-d_6, 298 K) δ = 8.87 (s, 1H), 8.45 (s, 1H), 5.92 (ddt, *J* = 17.3, 10.4, 5.3 Hz, 1H), 5.21 (dd, *J* = 17.2, 1.8 Hz, 1H), 5.12 (dd, *J* = 10.2, 1.7 Hz, 1H), 3.94 (ddd, *J* = 7.4, 4.6, 1.7 Hz, 2H).

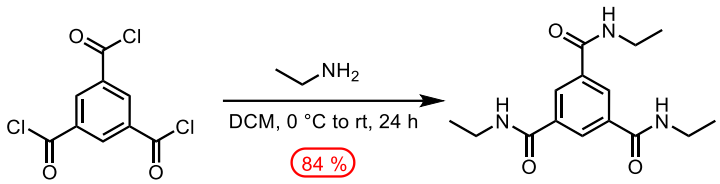

Scheme S3. Synthesis of triethyl benzamide (TEB)

TEB. Ethylamine (0.85 g, 9.5 mL 2M in THF, 18.8 mmol, 5 *equiv*.) was dissolved in anhydrous CH_2Cl_2 (30 mL) and the solution was cooled to 0 °C. To it, 1,3,5-benzenetricarbonyl trichloride (1.0 g, 3.76 mmol, 1.0 *equiv*.) in CH_2Cl_2 (5 mL) was added dropwise under stirring conditions. Then, the reaction mixture was stirred at room temperature for 24 h. Then, the CH_2Cl_2 was removed under reduced pressure and the crude product was washed with 0.5 N HCl (100 mL) followed by washing with saturated sodium bicarbonate

solution (100 mL). Finally, the product was washed with water and air-dried to afford TEB as a white powder (0.92 g, 3.15 mmol, yield 84 %).
^{1}H NMR (500 MHz, DMSO-d_6, 298 K) δ = 8.68 (t, J = 5.5 Hz, 1H), 8.37 (s, 1H), 3.35 – 3.27 (m, 3H), 1.14 (t, J = 7.2 Hz, 3H).

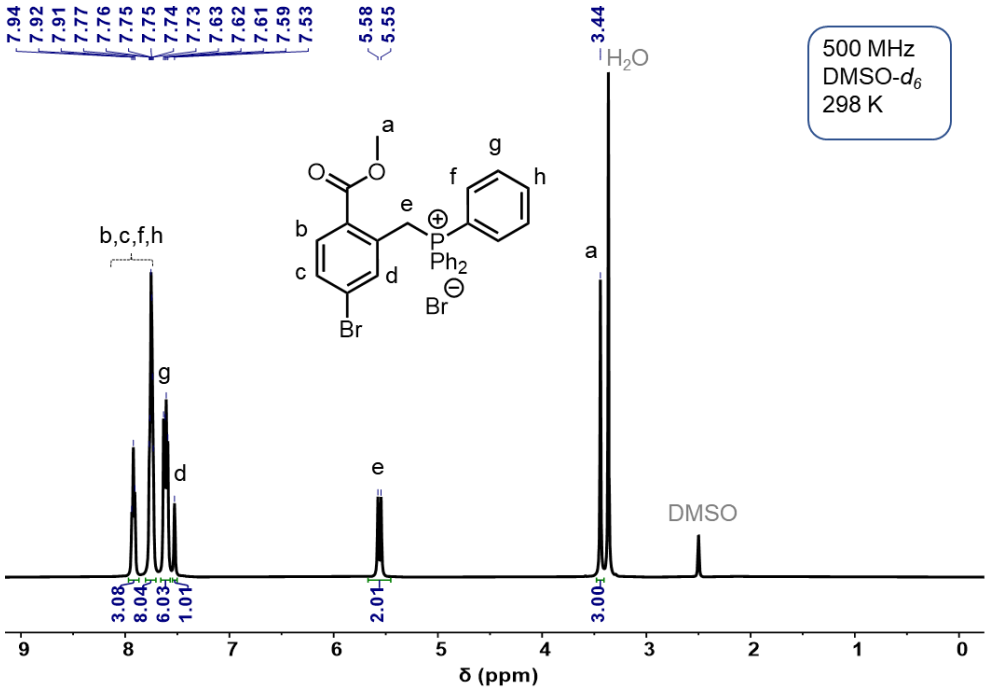

Figure S1. ^{1}H NMR spectrum of **1a** in DMSO-d_6 at 298 K

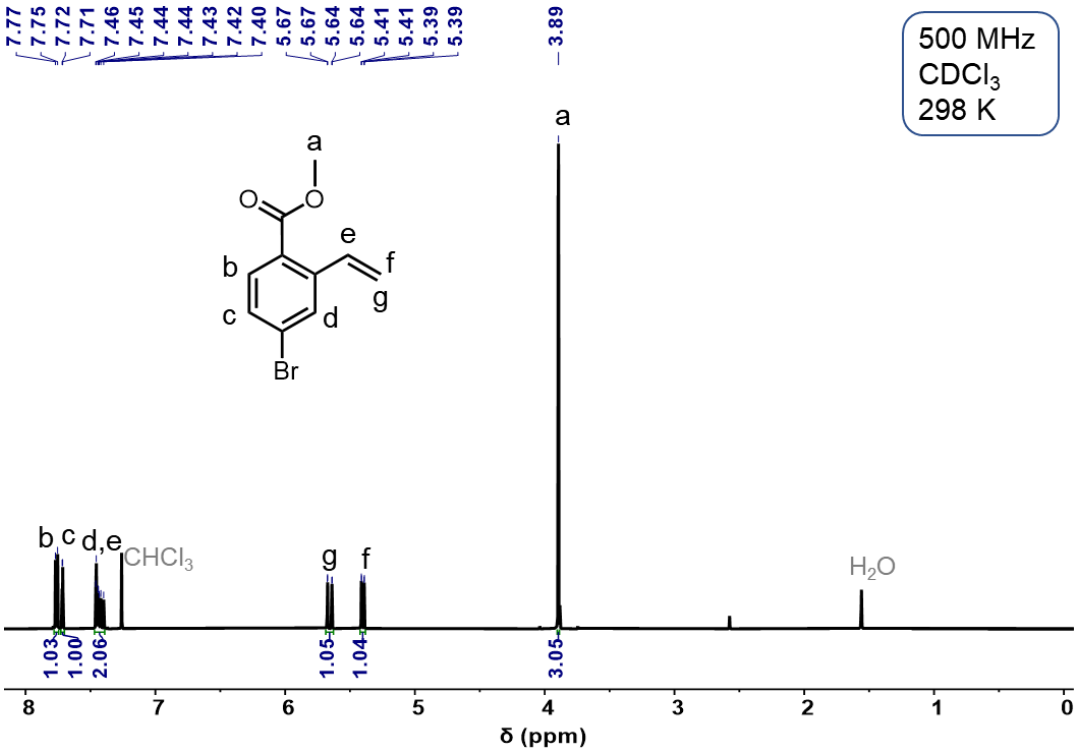

Figure S2. ^{1}H NMR spectrum of **1b** in $CDCl_3$ at 298 K

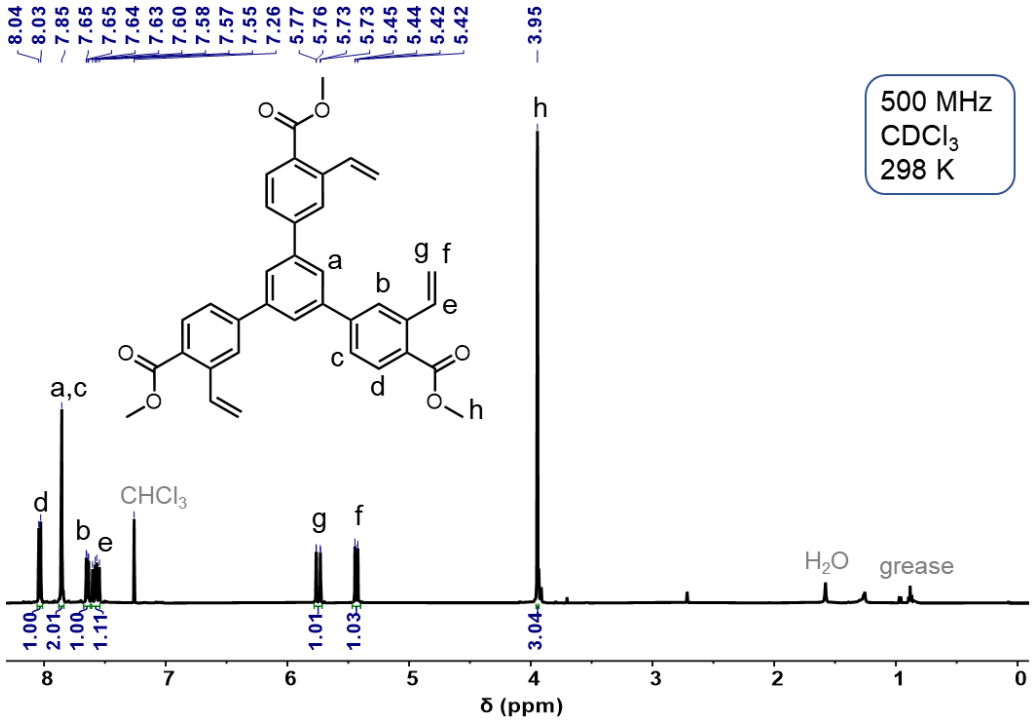

Figure S3. ^{1}H NMR spectrum of **1c** in $CDCl_3$ at 298 K

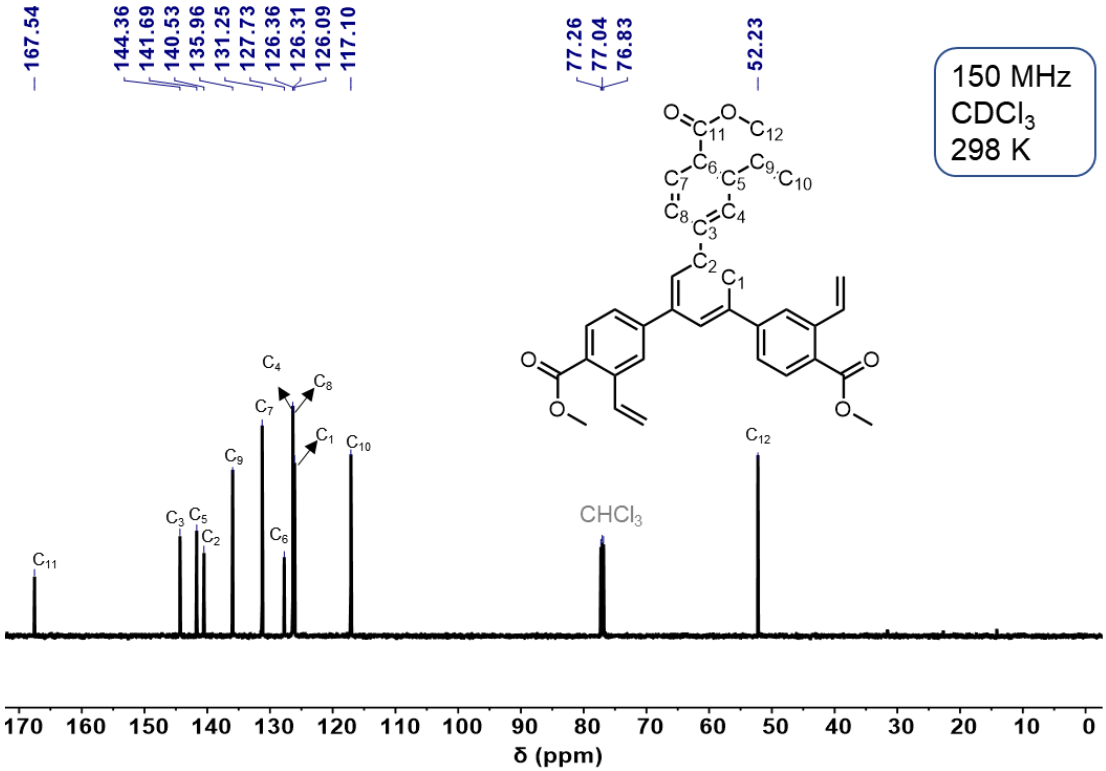

Figure S4. ^{13}C NMR spectrum of **1c** in $CDCl_3$ at 298 K

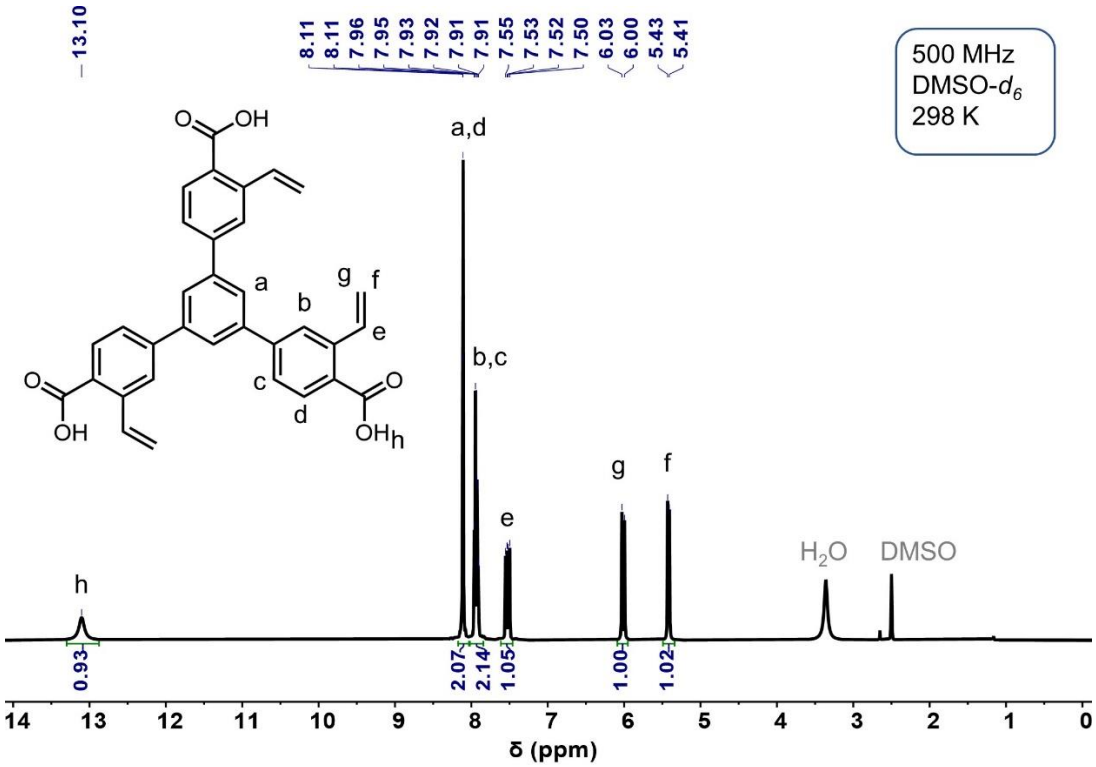

Figure S5. ^{1}H NMR spectrum of **1** in DMSO-d_6 at 298 K

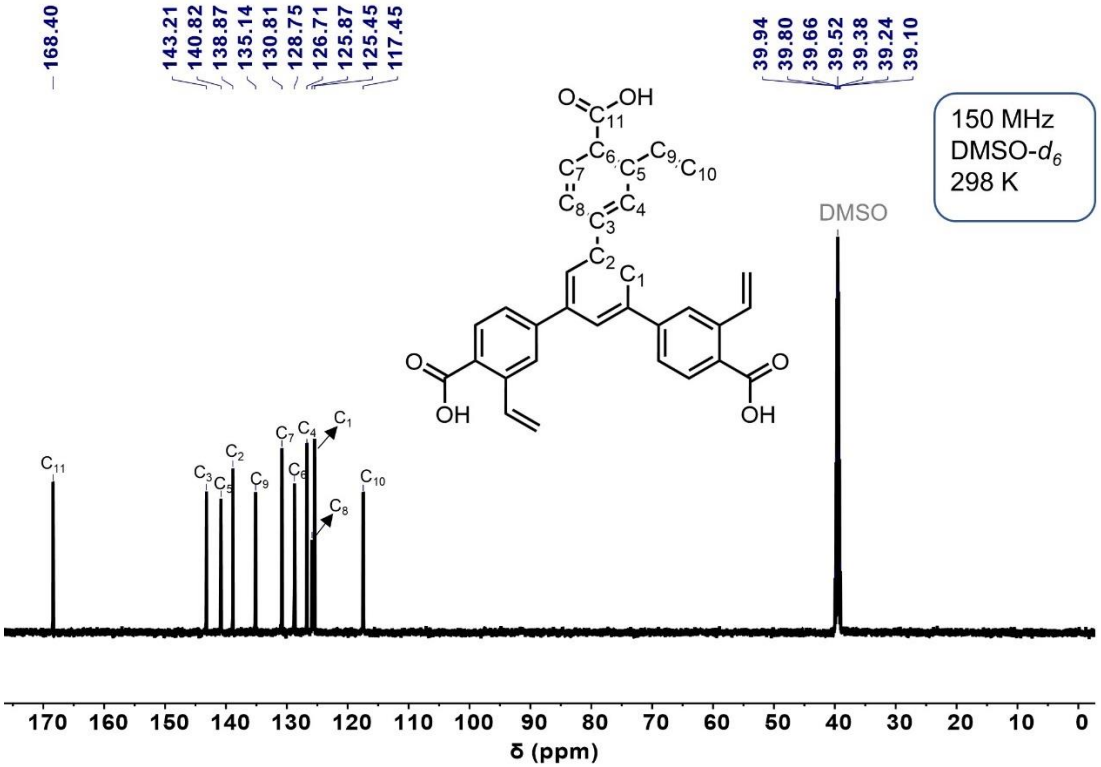

Figure S6. ^{13}C NMR spectrum of **1** in DMSO-d_6 at 298 K

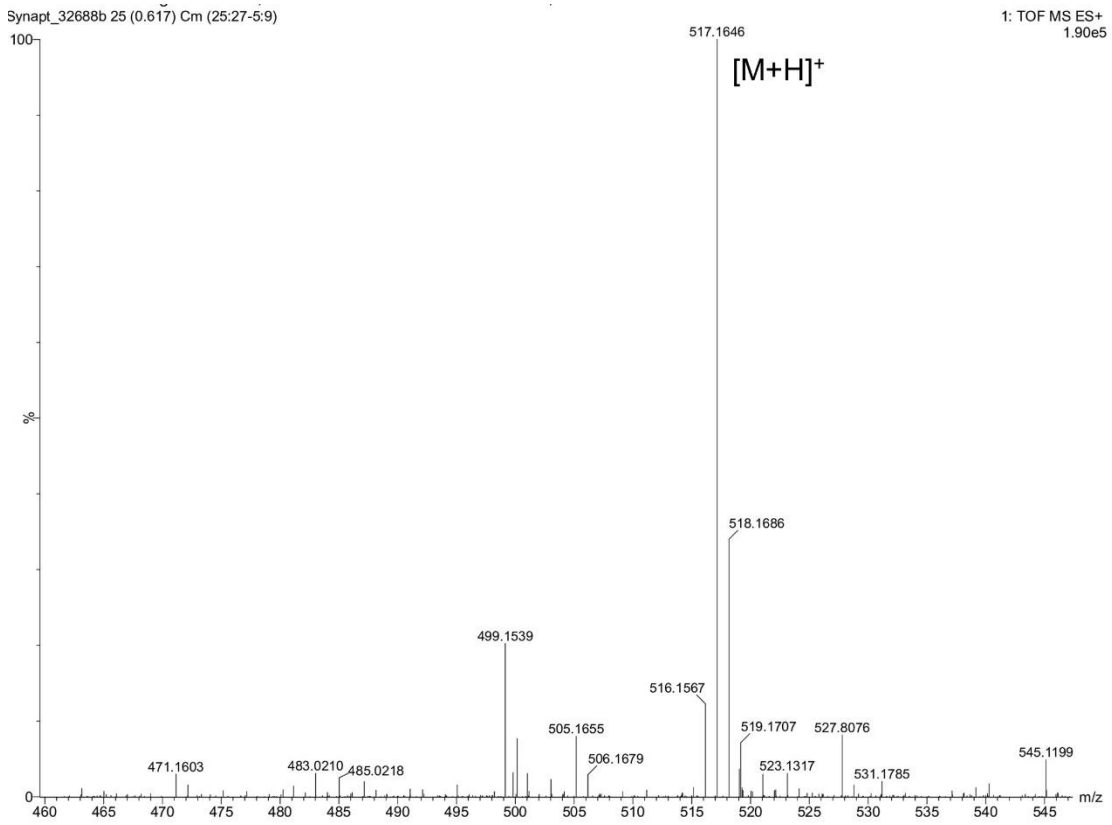

Figure S7. ESI-HRMS spectrum of **1**

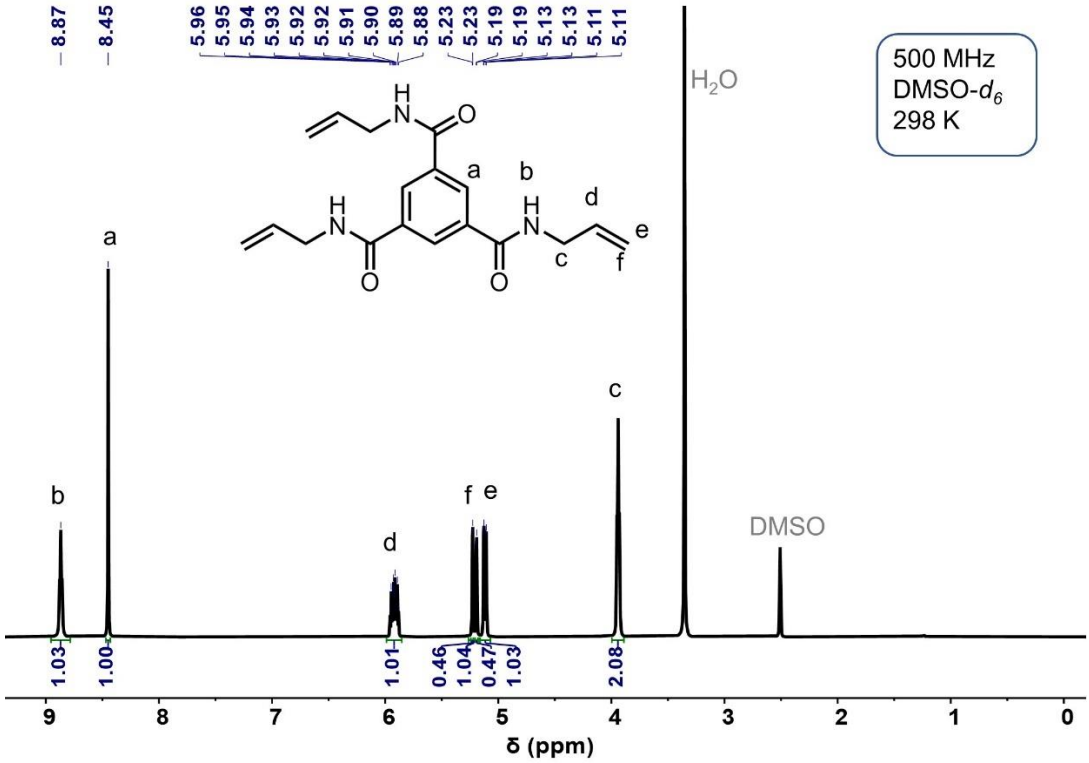

Figure S8. ^{1}H NMR spectrum of **TAB** in DMSO-d_6 at 298 K

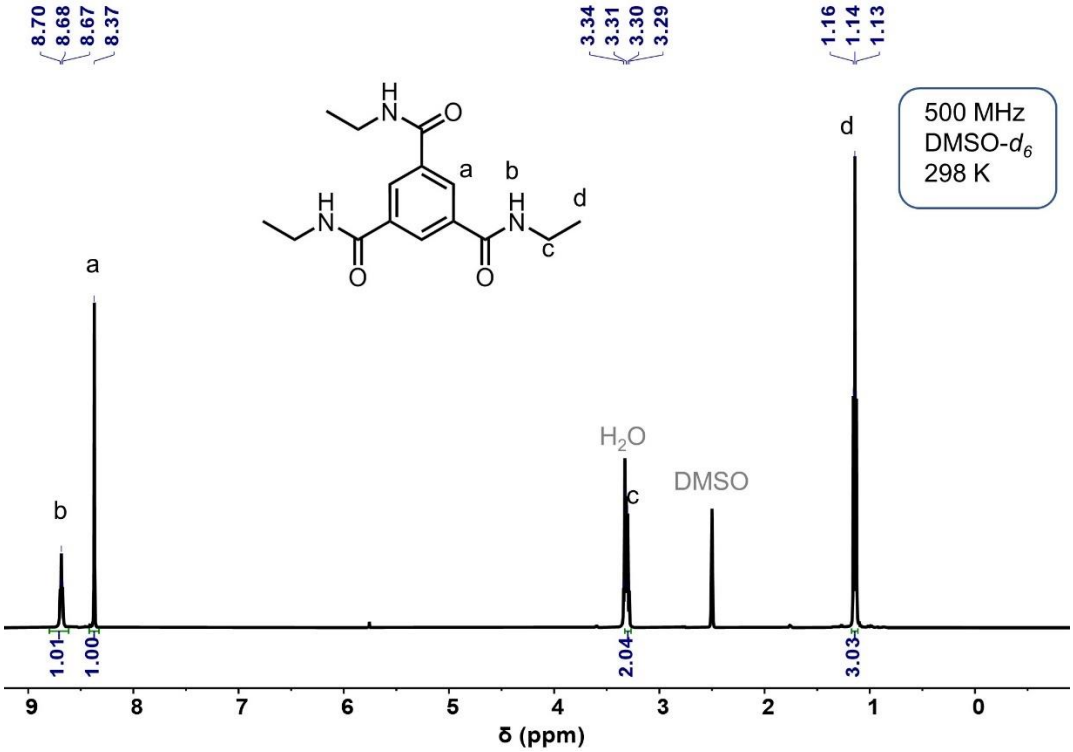

Figure S9. ^{1}H NMR spectrum of **TEB** in DMSO-d_6 at 298 K

S3. Synthesis and Characterizations of H_COFs

Co-crystallization of 1 and TAB. High-quality single crystals of **1**•TAB were obtained by slow diffusion of hexane into a 1,4-dioxane solution (10 mL) of **1** (50.0 mg, 96.8 μmol) and TAB (31.6 mg, 96.8 μmol, 1.0 *equiv*. to **1**) at room temperature for 7 days. **1**•TAB**:** 62 mg, 76% yield.

Encapsulation of isoprene in 1•TAB crystals. 1•TAB crystals were dried under vacuum for 48 h to completely remove the crystallization solvents from the pores and soaked in neat isoprene for another 8 h in a vial. Then a few crystals were isolated from the vial and dried over absorbent paper to remove surface-absorbed isoprene. These crystals were then dissolved in DMSO-d_6 for NMR analysis, which shows the presence of isoprene inside the crystals. We didn't investigate the encapsulation of butadiene because it is a gaseous substrate.

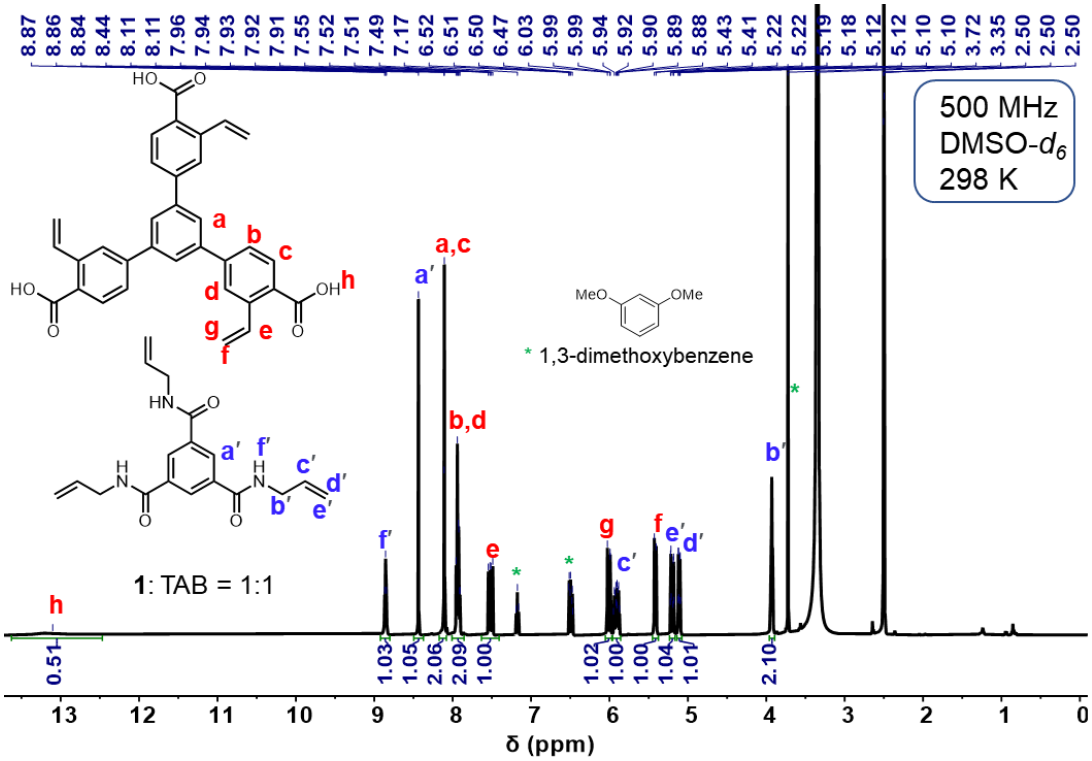

Figure S10. ^{1}H NMR spectrum of the dissolved **1**•TAB crystals in DMSO-d_6 at 298 K.

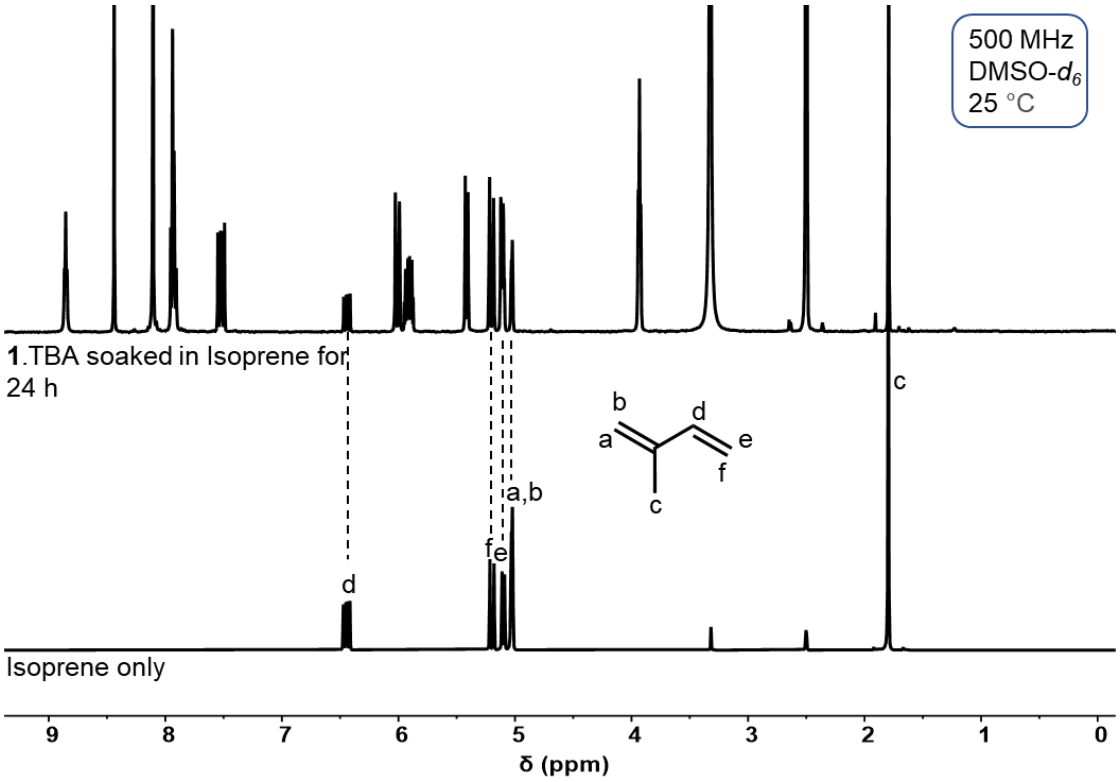

Figure S11. ^{1}H NMR spectrum of encapsulated isoprene in **1**•TAB crystals in DMSO-d_6 at 298 K.

Synthesis of single-crystalline H_COF-106 and H_COF-107.

Several concentrations of isoprene or butadiene were tested for the synthesis H_COFs. First, mother liquid of **1**•TAB was removed, and the crystals were washed three times using hexane (5 mL × 3) and dried in the open air. Then, a seriers of diluted solution (from 1% to 10%, v/v) of isoprene or butadiene were prepared in hexane in glass vials and **1**•TAB crystals along with 2,2-dimethoxy-2-phenylacetophenone (radical initiator, 0.04 mol %) were added. The vials were kept in the dark for 24 h to allow thorough diffusion of butadiene or isoprene. The vials were then irradiated under UV light (medium-pressure 175-watt Hg lamp) for 72 h with forced air cooling. The crystal samples were collected and washed with an excess of hexane to remove the unreacted butadiene or isoprene and then dried under vacuum. However, at these concentrations, the yield of the H_COFs were low (below 50%) because the diffusion of the crosslinkers into the pores of the crystals was not as effective due to competition between the solvents and the crosslinkers. Then we targeted to maximize the yield of the H_COFs, so we used neat isoprene and a high concentration of butadiene (15% v/v in hexane) for the crosslinking reactions for H_COF-106 and H_COF-107, respectively.

Synthetic procedure. Mother liquid of **1**•TAB was removed, and the crystals were washed three times using hexane (5 mL × 3) and dried in the open air. **1**•TAB crystals (50 mg) in a 20 mL glass vial were charged with 1,3-butadiene (15 mL, 15 wt. % in hexane), 2,2-dimethoxy-2-phenylacetophenone (radical initiator, 0.04 mol %) and CCl_4 (3 mL). Here, CCl_4 was added to enhance the solubility of all reagents. The vial was kept in the dark for 24 h to allow thorough diffusion of butadiene. The vial was irradiated under UV light (medium-pressure 175-watt Hg lamp) for 72 h with forced air cooling. The crystal samples were collected and washed with an excess of hexane to remove the unreacted butadiene and then dried under vacuum to obtain H_COF-106 crystals.

The H_COF-107 was synthesized following similar reaction conditions except CCl_4 was not required in this case. **1**•TAB crystals (50 mg) in a 20 mL glass vial were charged with isoprene (10 mL) and 2,2-dimethoxy-2-phenylacetophenone (0.04 mol %).

These crystal samples were activated using supercritical CO_2 and used for the different analyses.

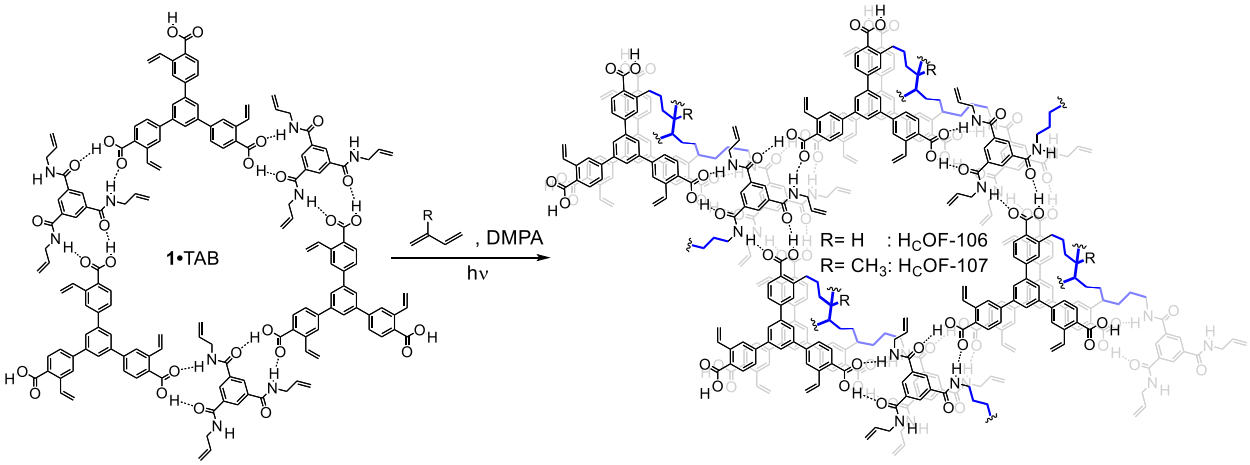

Scheme S4. Single-crystal to single-crystal (SCSC) transformation of **1**•TAB crystal to H_COF-106 and H_COF-107.

^{1}H NMR analysis of the residues. After crosslinking, the excess isoprene was decanted, and the crystals were washed multiple times with hexane. The crystals were immersed in DMSO-d_6 and heated to boiling for 1-2 min before cooling down, and the sample was subjected to NMR analysis. Under the microscope, A majority of the crystals remained undissolved. To quantify the amount of undissolved samples, the mass of the DMSO-treated samples was recorded. For 20 mg of **1**•TAB used for crosslinking, the mass of the obtained H_COF-106 and H_COF-107 were measured as 13 mg and 15 mg with 63% and 72% yields, respectively. Molecular weights are calculated according to the asymmetric unit of the crystal: 1•TAB: 1687.87 g/mol, HCOF-106: 1745 g/mol, and H_COF-107: 1760 g/mol.

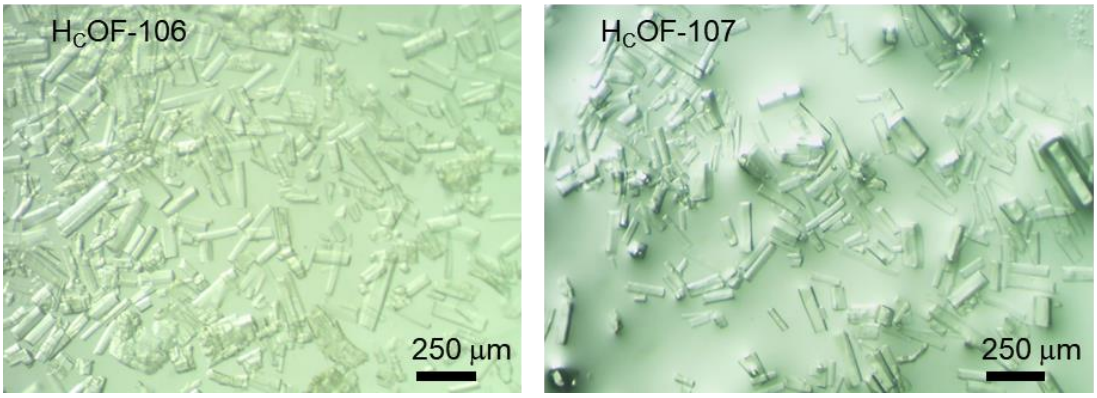

Figure S12. Images of H_COF-106 and H_COF-107 crystals after DMSO treatment.

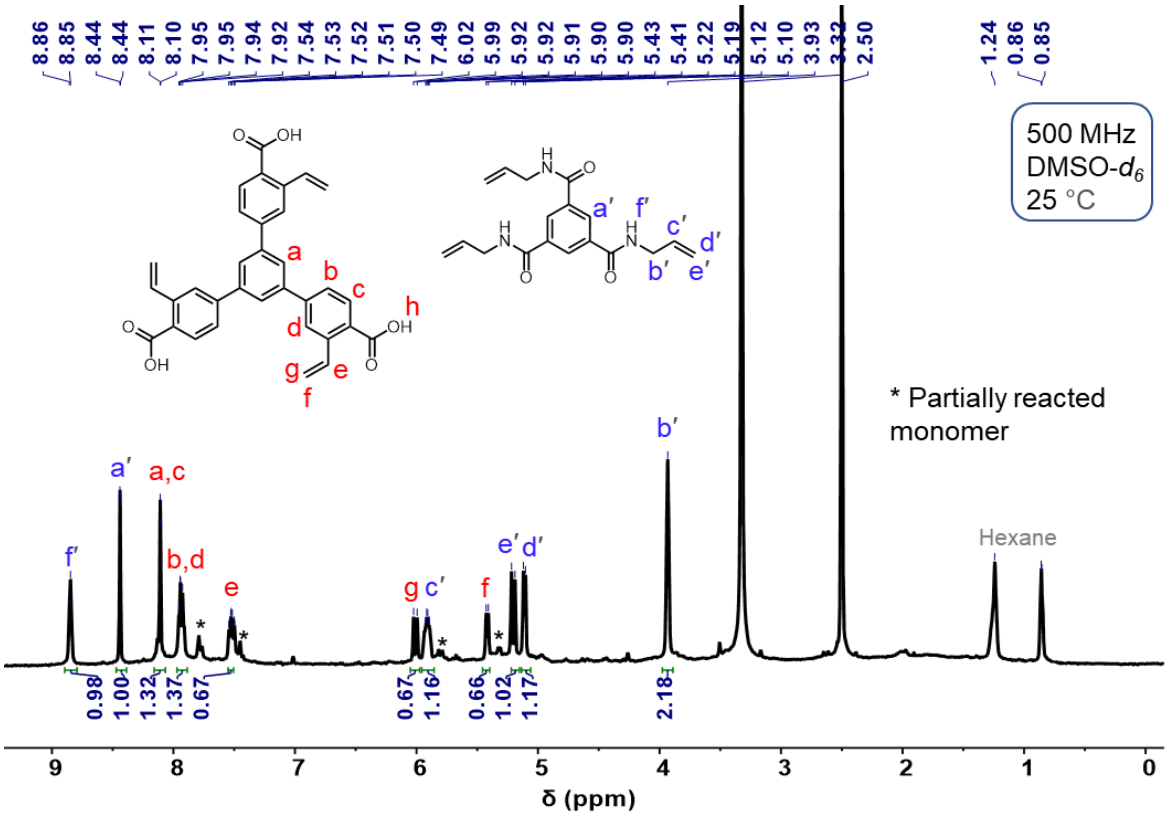

Figure S13. ^{1}H NMR spectrum of H_COF-106 residue in DMSO-d_6 at 298 K.

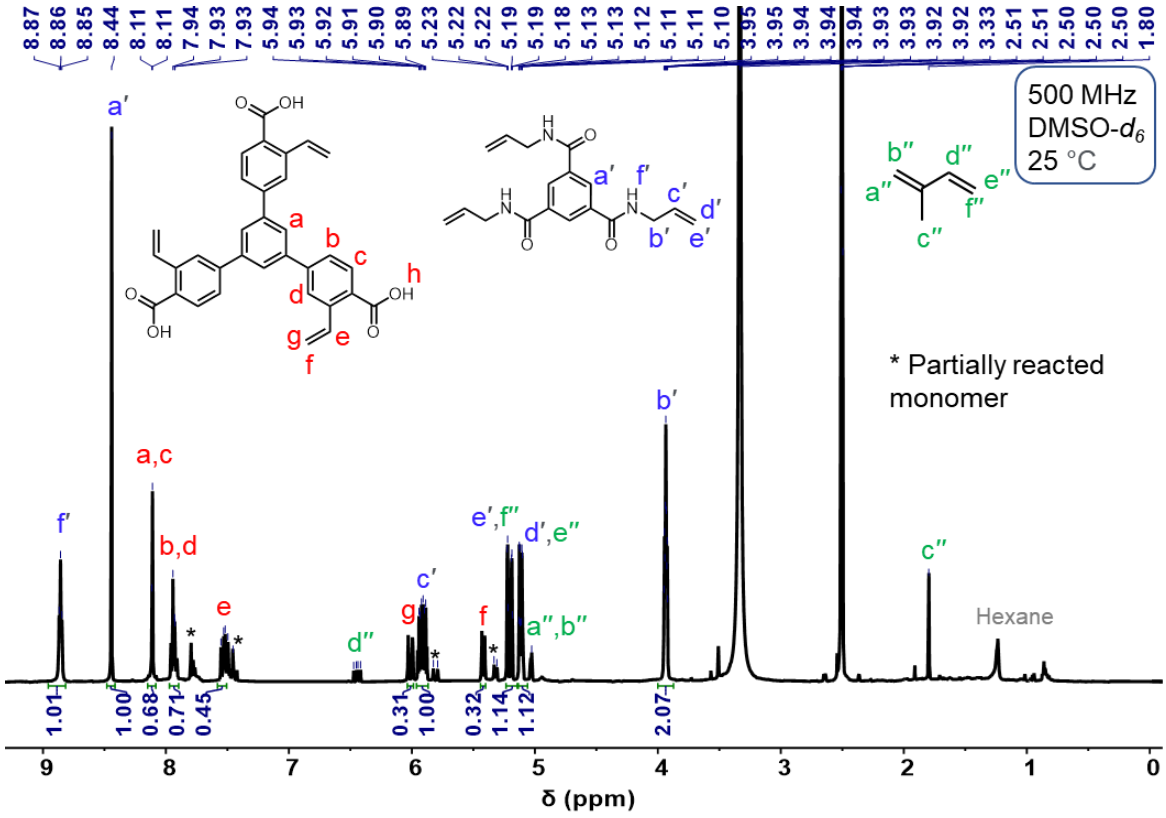

Figure S14. ^{1}H NMR spectrum of H_COF-107 residue in DMSO-d_6 at 298 K.

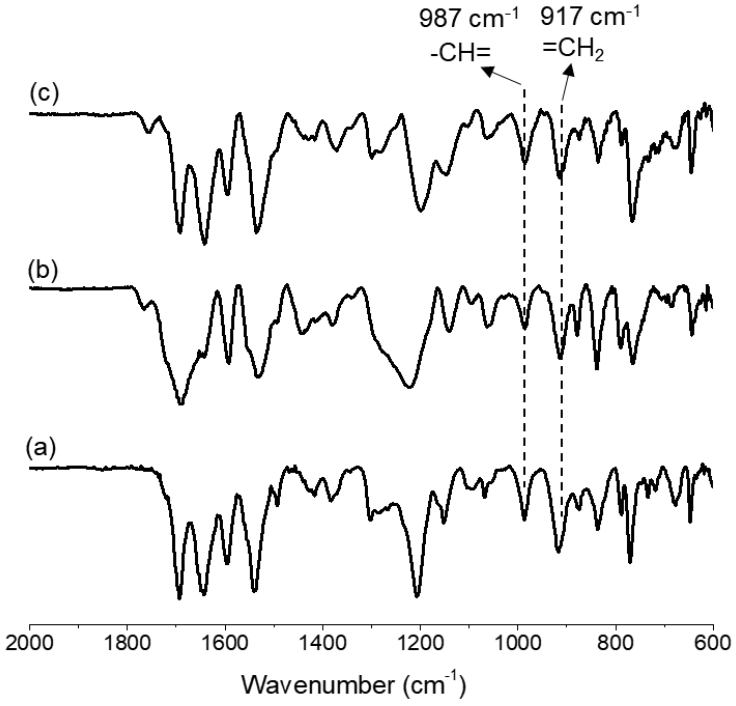

Figure S15. FT-IR spectra of (a) **1**•TAB, (b) H_COF-106, and (c) H_COF-107 after DMSO treatment.

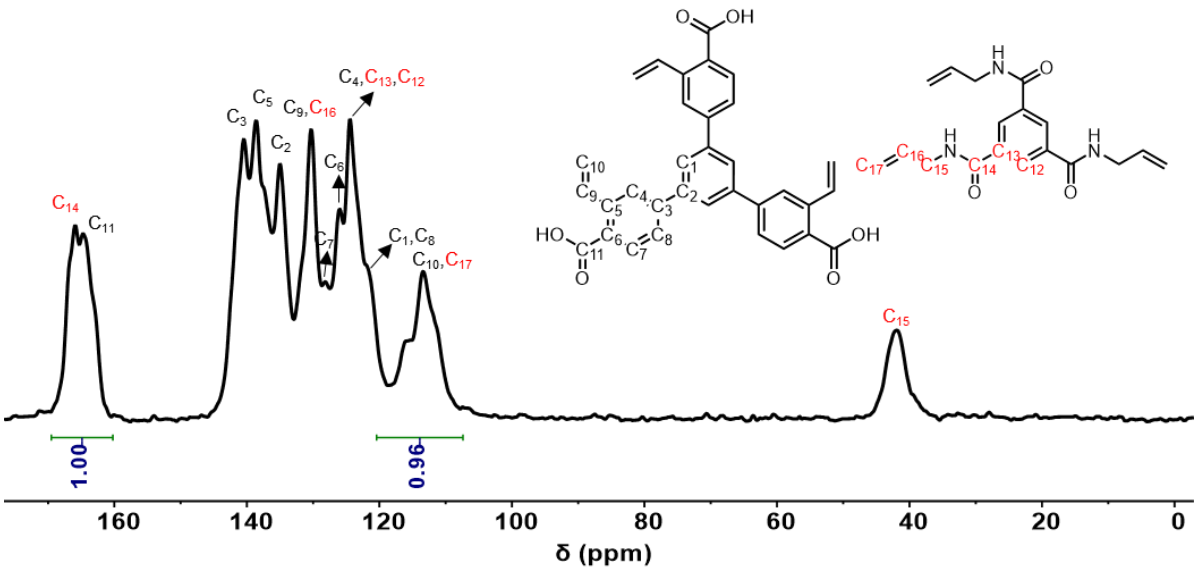

Figure S16. Solid-state ^{13}C NMR spectrum of **1**•TAB.

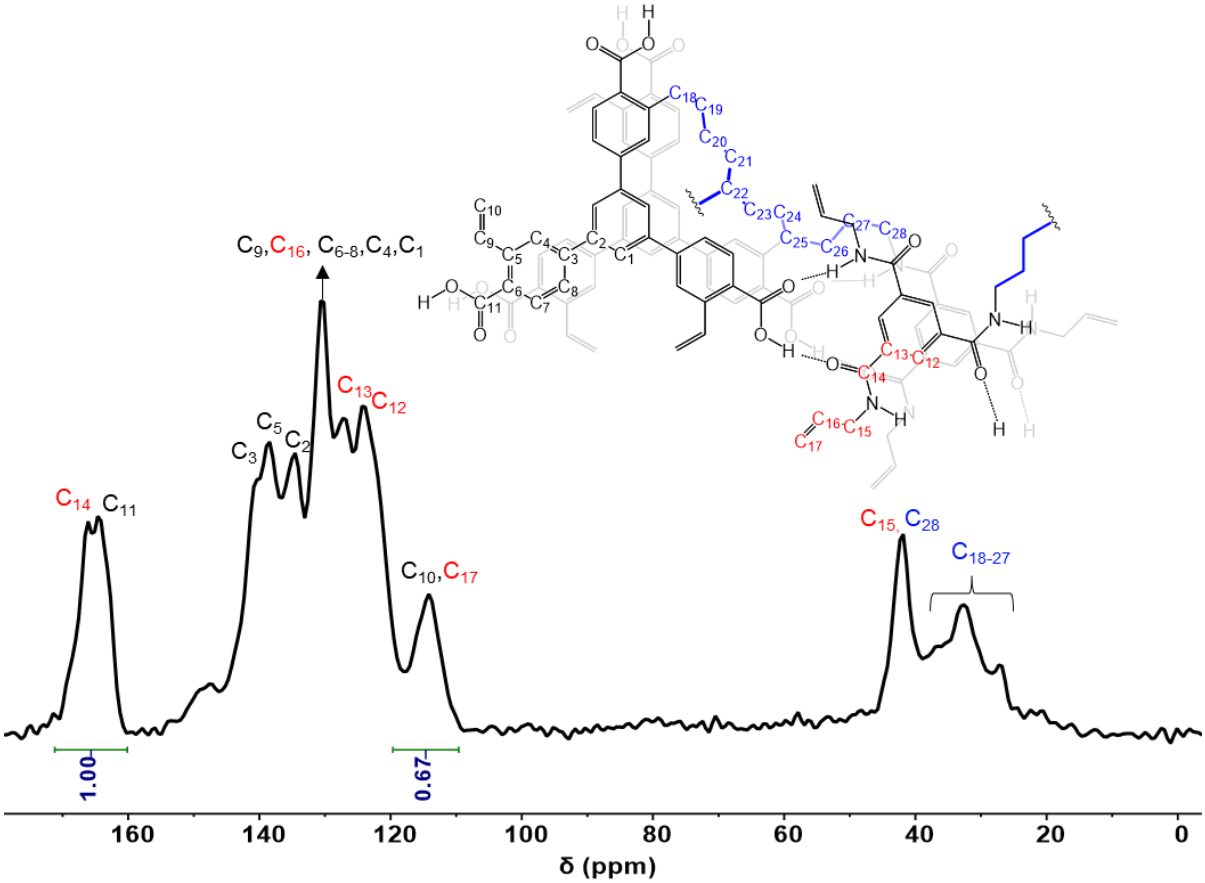

Figure S17. Solid-state ^{13}C NMR spectrum of H_COF-106.

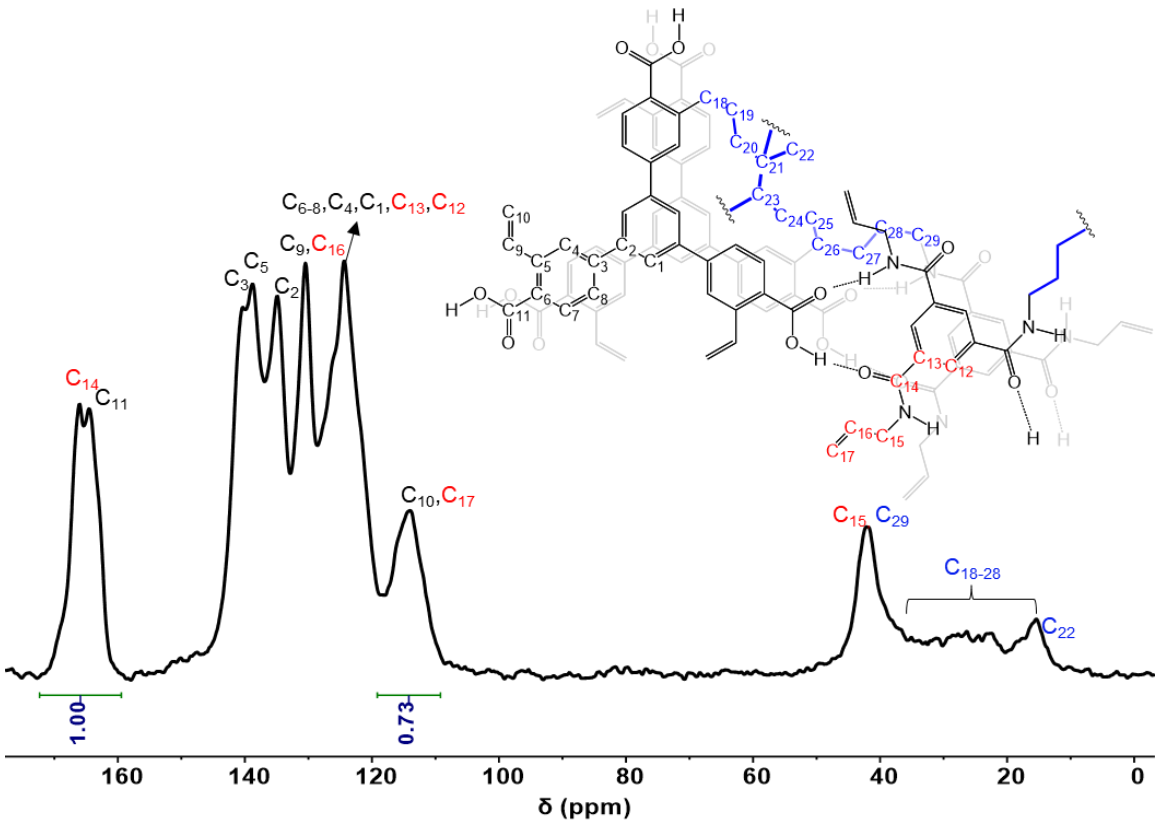

Figure S18. Solid-state ^{13}C NMR spectrum of H_COF-107.

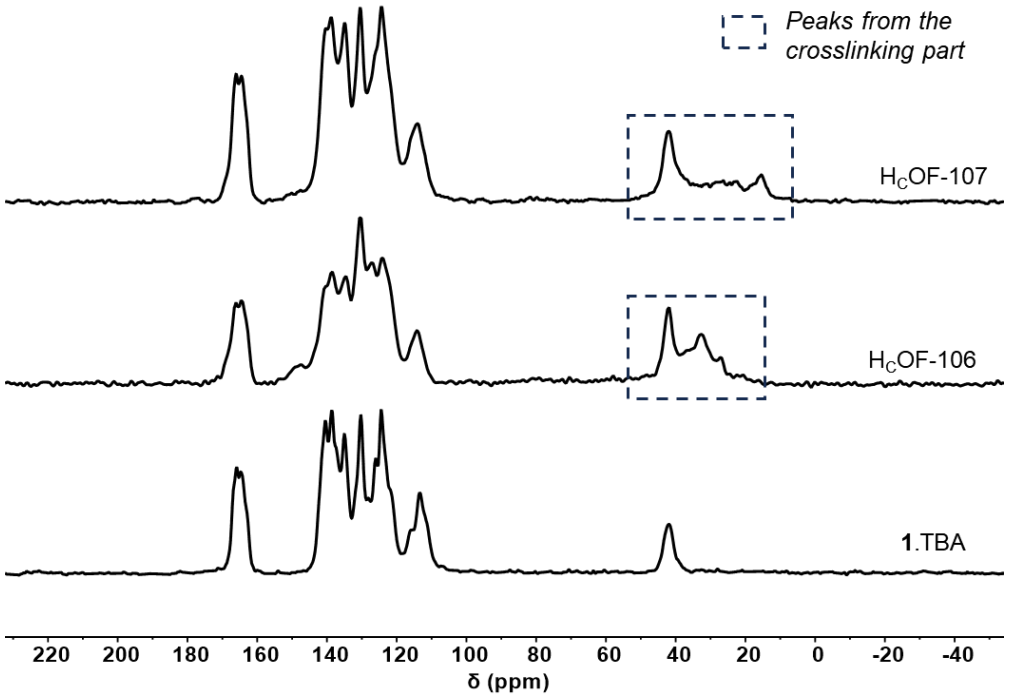

Figure S19. Comparison of Solid-state ^{13}C NMR spectra for **1**•TAB, H_COF-106 and H_COF-107.

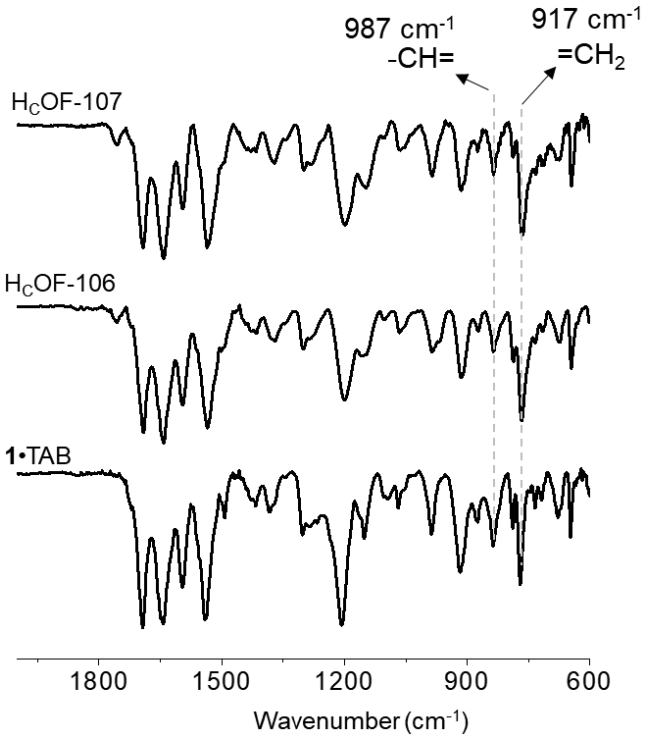

Figure S20. Stacked FT-IR spectra of **1**•TAB, H_COF-106, and H_COF-107.

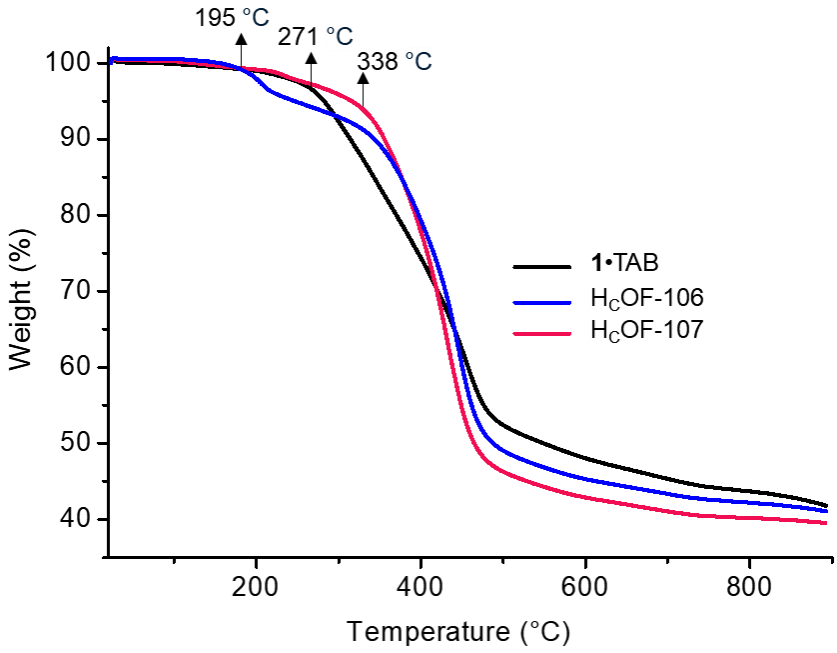

Figure S21. TGA profiles for **1**•TAB, H_COF-106, and H_COF-107.

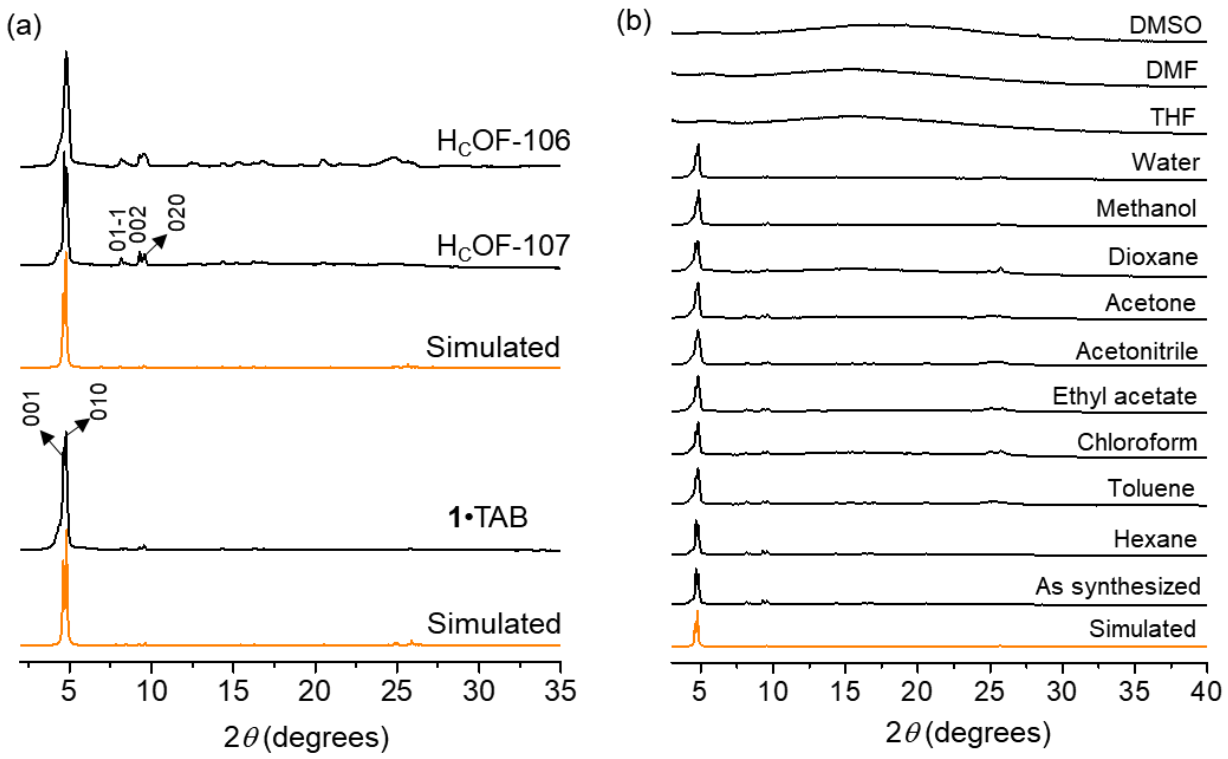

Figure S22. Simulated and experimental PXRD profiles of **1**•TAB, H_COF-106, and H_COF-107. (b) PXRD profiles of H_COF-107 in different solvents.

Table S1. Elemental Analysis

Sample	Composition found from elemental analysis	Calc.	Found.
H_COF-106	[**1**•TAB]$_2$, **[Butadiene]**$_{1.1}$, [H_2O]$_{2.05}$	C 71.62, H 5.69, N 4.71	C 70.7, H 5.79, N 4.18
H_COF-107	[**1**•TAB]$_2$, **[Isoprene]**$_{1.15}$, [H_2O]$_{0.25}$	C 73.09, H 5.68, N 4.75	C 73.67, H 5.78, N 4.17

Determination of the number of free olefins present in 1•TAB and H_COF-107 using the Iodine value test (Wijs method).[6]

Standard solutions prepared:

1. 250 mL 0.1 N sodium thiosulfate (aqueous solution)
2. 50 mL 30 % KI (aqueous solution)
3. 10 mL 1 % starch (aqueous solution)

The **1**•TAB crystals (32 mg) were taken in $CHCl_3$ (2 mL) in a 50 mL screw cap glass bottle and to it Wijs solution (3 mL, Iodine monochloride, approx. 0.22 N soln. in glacial acetic acid) was added. Then the sample was kept in the dark for 24 h. A blank was prepared with $CHCl_3$ (2 mL) and Wijs solution (3 mL)

in another 50 mL screw cap glass bottle and kept in the dark for the same time as for the sample. Next, 30 % KI solution (1.5 mL) was added to the reaction mixture to convert unreacted ICl to iodine. Then water (20 mL) was added to dilute the solution and it was immediately titrated with 0.1 N sodium thiosulfate using 1 % starch (1 mL) as an indicator. The same process was repeated for the blank as well. The iodine value was determined using the following formula.

$$\text{Iodine value (IV): } [(B - S) \times N \times 12.6]/ W \qquad \ldots \text{Eq 1}$$

- (B – S): The difference between the volumes, in mL, of sodium thiosulfate required for titrating the blank and the sample, respectively.
- N: Normality of sodium thiosulfate solution.
- 12.69: The conversion factor from mEq sodium thiosulfate to grams of iodine (the molecular weight of iodine is 126.9 g/mol)
- W: Weight of the sample in grams.

Similar experiments were conducted for H_COF-107 (50 mg). The measured iodine value for **1**•TAB is 181.13, and 88.2 for H_COF-107.

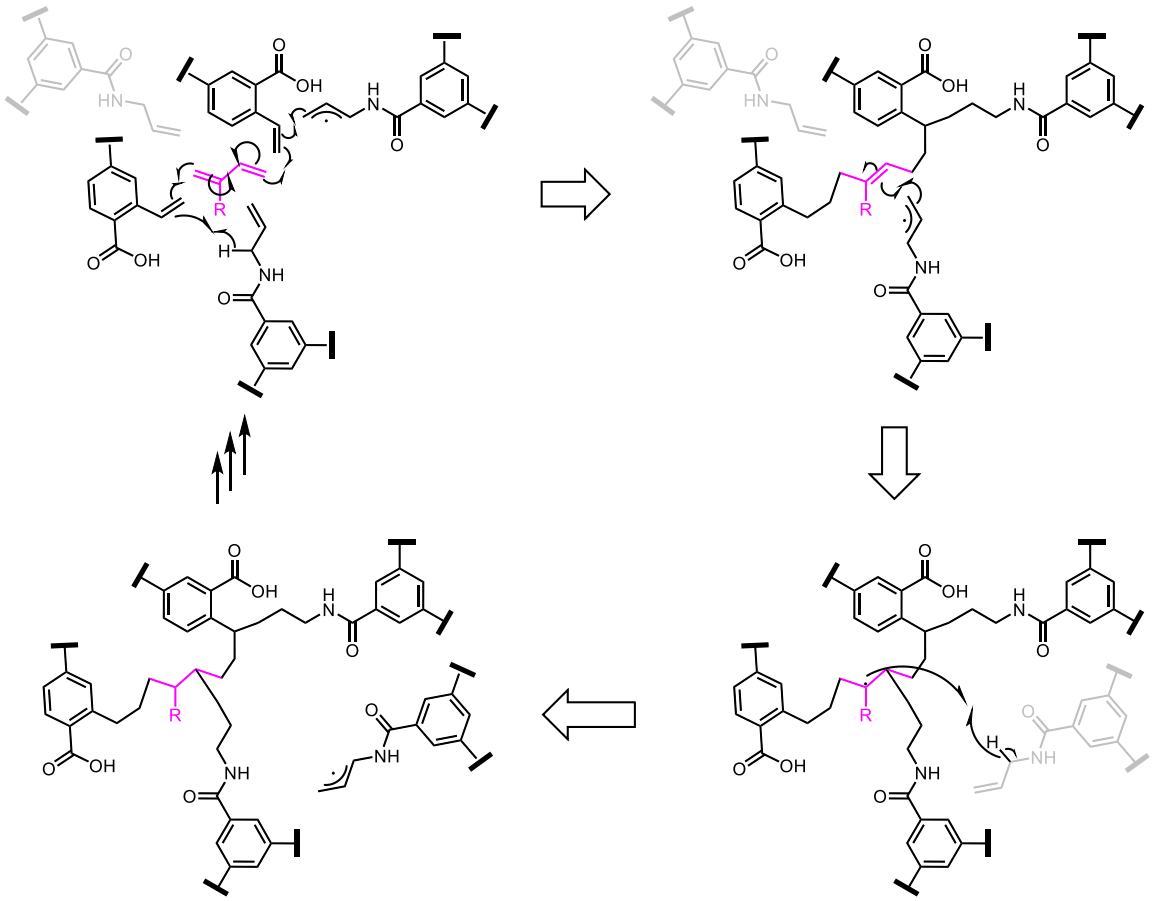

Scheme S5. The plausible radical crosslinking took place between styrene, isoprene(/butadiene), and TAB. *Note*: Here the crosslinking reaction is successful as the size of the olefinic crosslinker is suitable to facilitate radical propagation and the generated radical possess sufficient reactivity (comparable pKa values) to effectively participate in reactions with styrene or allyl moieties.

Test for diene polymerization outside H_COFs. During the photoreaction, only a small amount of polyisoprene or polybutadiene was observed. After the reaction (72 h), 5 μl of the supernatant residual isoprene (or butadiene) was taken in $CDCl_3$ for the NMR analysis.

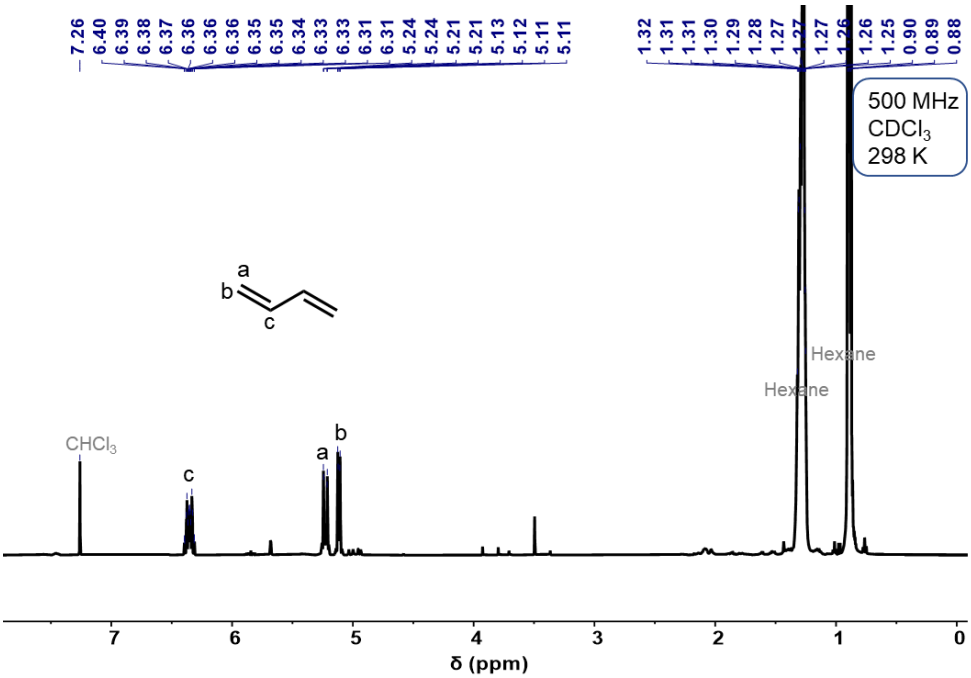

Figure S23. ^{1}H NMR spectrum of residual butadiene (15% in hexane) in $CDCl_3$ at 298 K.

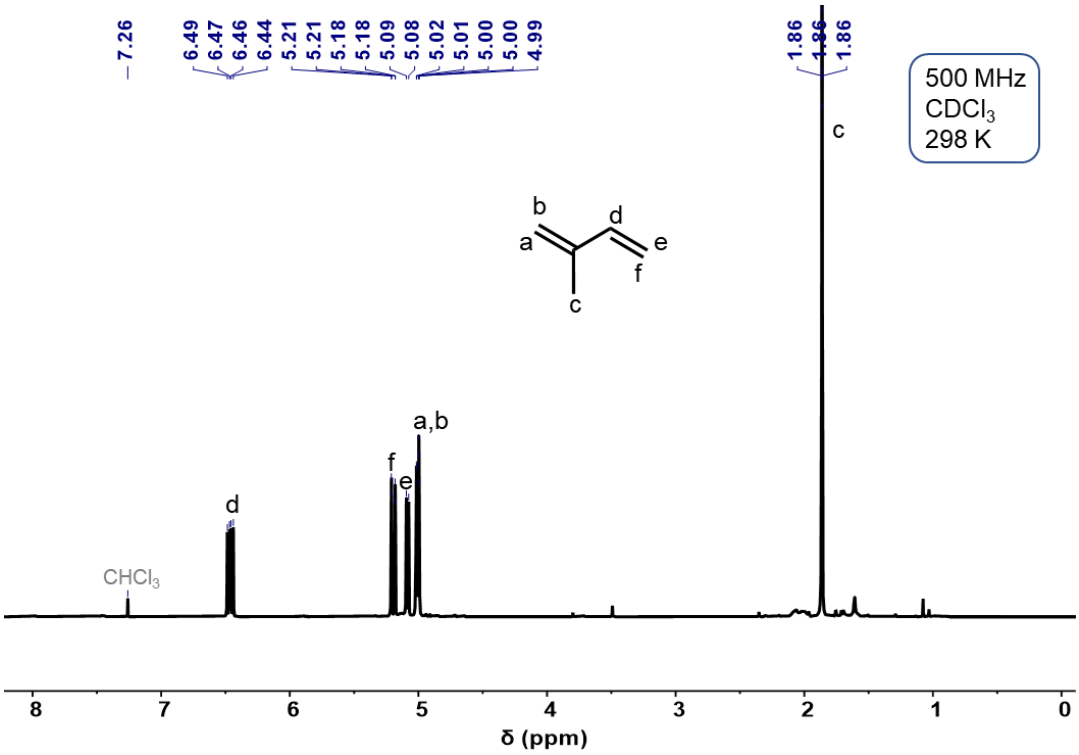

Figure S24. ^{1}H NMR spectrum of residual isoprene in $CDCl_3$ at 298 K.

Activation and sorption analysis. The **1**•TAB and Iso-H_COF crystals were kept under vacuum for 48 h. Then the samples were placed in the drying chamber, which was filled with CO_2. The CO_2 input was maintained for an additional 15 min to purge the chamber. Next, the chamber was sealed, and the temperature was raised to 40 °C (above the critical temperature of CO_2) with an inlet pressure of 1000 psi. These conditions were held overnight to afford the activated crystal samples. The supercritical CO_2 activation was repeated two times. Low-pressure gas/vapor sorption measurements were performed on a Micrometritics FLEX 3.0 surface area analyzer. Samples were degassed under a dynamic vacuum for 8 h at 70 °C before each measurement. The N_2 sorption isotherm was measured using a liquid nitrogen bath (77 K). The CO_2 sorption isotherm was measured using an ice bath (273 K) and a dry ice bath (195 K). Solvent vapor sorption isotherms were measured at room temperature (297 K).

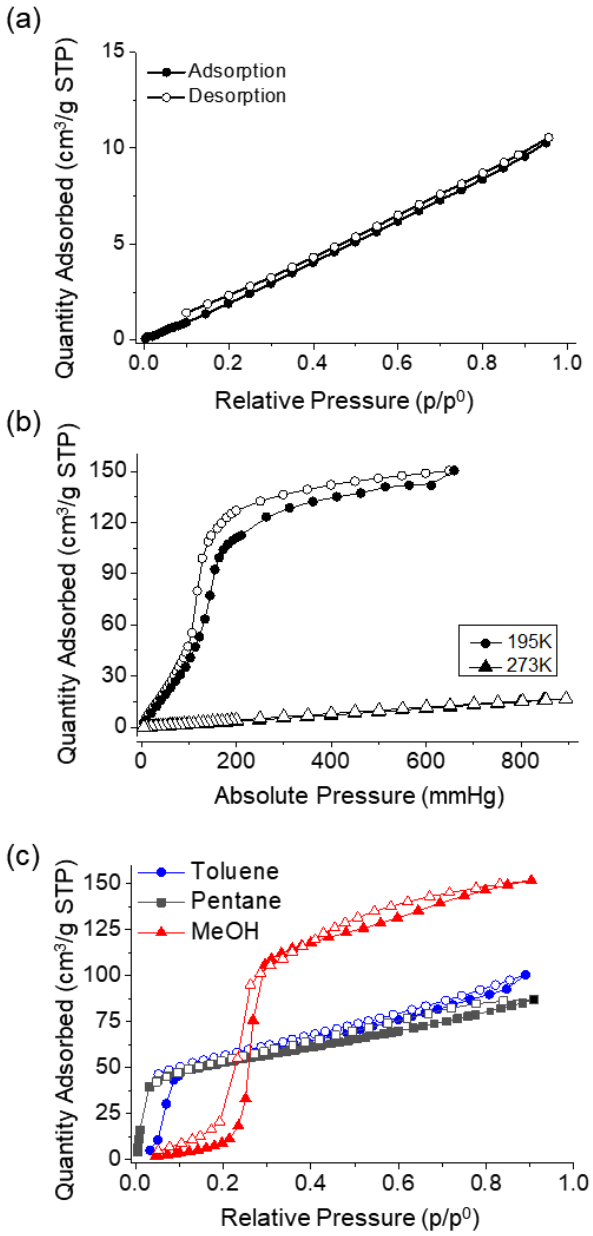

Figure S25. Gas sorption isotherm (a) N_2 and (b) CO_2 and solvent vapor sorption isotherms (c) of **1**•TAB.

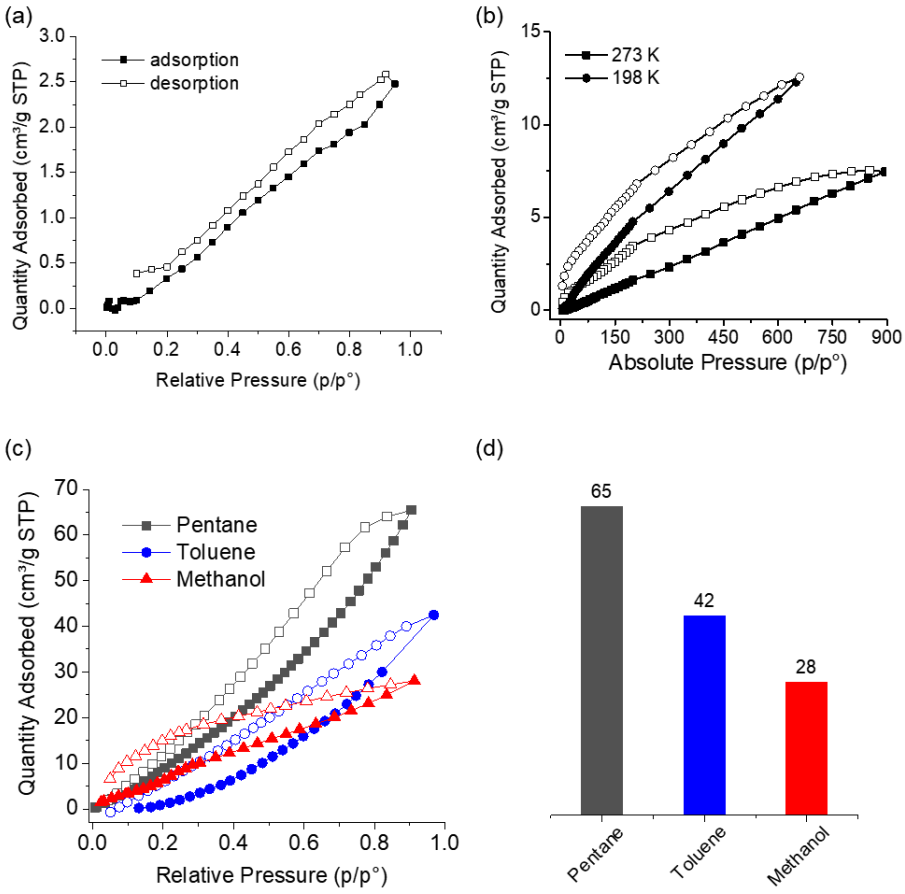

Figure S26. (a) N_2 and (b) CO_2 gas sorption of H_COF-107. (c) and (d) solvent vapor sorption isotherms of H_COF-107; Pentane (black), toluene (blue), and methanol (red).

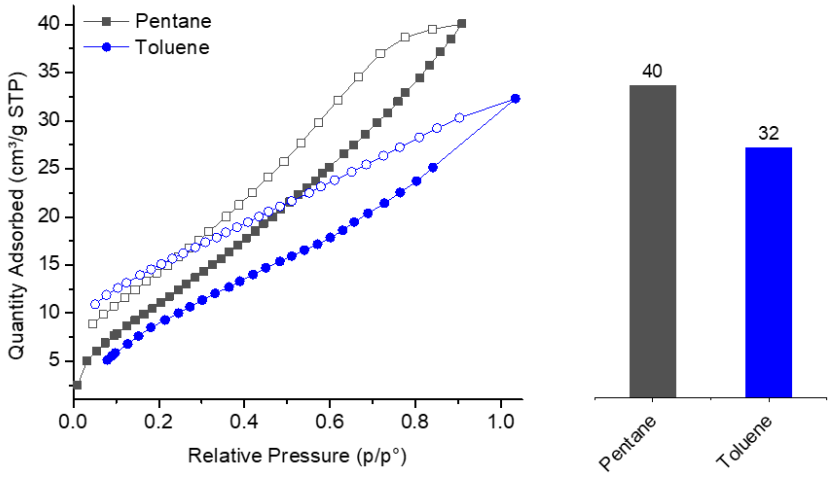

Figure S27. Solvent vapor sorption isotherms of H_COF-106; Pentane (black) and toluene (blue).

S4. Single crystal X-ray crystallography

Single crystal X-ray diffraction data for **1**•TAB, **1**•TEB, H_COF-106, and H_COF-107 were collected on a Rigaku Synergy dualflex diffractometer with CuKα radiation at 100 K. Preliminary lattice parameters and orientation matrices were obtained from three sets of frames. Then the full data were collected using the ω and ϕ scanning method with a frame width of 0.5°. These data were processed with the Rigaku CrisalisPro software[7] package. Multiscan absorption corrections were applied in each case. The structures were solved by SHELXT[8] and refined with SHELXL[9] using an Olex2 program.[10] Similar 1,2 and 1,3 bond length (SADI), fixed bond length (DFIX), similar Uij (SIMU), and rigid body (RIGU) restraints were applied wherever necessary. Hydrogen atom positions were calculated geometrically and refined using the riding model. For all the crystals, the scattered electron density in the model cannot be modeled in a meaningful manner, which was removed using the "solvent mask" implemented in Olex2.

Table S2. Single crystal X-ray diffraction data of **1**•TAB, **1**•TEB, H_COF-106, and H_COF-107.

Identification code	**1**•TAB	**1**•TEB	H_COF-106	H_COF-107
CCDC number	2347283	2347284	2347292	2347291
Empirical formula	$C_{102}H_{90}N_6O_{18}$	$C_{144}H_{135}N_9O_{27}$	$C_{106}H_{92.03}N_6O_{18}$	$C_{107}H_{98.09}N_6O_{18}$
Formula weight	1687.79	2423.60	1737.88	1756.00
Temperature/K	100.15	100.00(10)	100.0(2)	99.98(11)
Crystal system	triclinic	monoclinic	triclinic	triclinic
Space group	$P\bar{1}$	$C2/c$	$P\bar{1}$	$P\bar{1}$
a/Å	14.3348(2)	38.1160(9)	14.4561(7)	14.4122(8)
b/Å	21.7619(3)	21.9306(4)	21.9459(8)	21.9201(8)
c/Å	21.9674(3)	42.5599(12)	22.0092(6)	22.0159(5)
α/°	114.6420(10)	90	60.305(3)	60.357(3)
β/°	97.6090(10)	103.440(2)	83.030(3)	83.564(3)
γ/°	108.0790(10)	90	74.276(4)	74.230(4)
Volume/Å^3	5642.85(14)	34601.8(14)	5837.8(4)	5815.3(5)
Z	2	8	2	2
ρ_{calc} g/cm^3	0.993	0.930	0.989	1.003
μ/mm^{-1}	0.558	0.527	0.552	0.557
F(000)	1776.0	10224.0	1828.0	1852.0
Crystal size/mm^3	0.15 × 0.04 × 0.04	0.29 × 0.1 × 0.1	0.1 × 0.02 × 0.02	0.1 × 0.03 × 0.03
Radiation	Cu Kα (λ = 1.54184)	Cu Kα (λ = 1.54184)	Cu Kα (λ = 1.54184)	Cu Kα (λ = 1.54184)
2Θ range for data collection/°	6.574 to 160.51	4.91 to 162.072	4.622 to 117.868	9.56 to 117.868
Index ranges	-18 ≤ h ≤ 17, -16 ≤ k ≤ 26, -27 ≤ l ≤ 28	-38 ≤ h ≤ 47, -27 ≤ k ≤ 27, -54 ≤ l ≤ 51	-16 ≤ h ≤ 16, -24 ≤ k ≤ 24, -24 ≤ l ≤ 24	-16 ≤ h ≤ 15, -23 ≤ k ≤ 24, -18 ≤ l ≤ 24
Reflections collected	91833	138822	66606	50666
Independent reflections	23959 [R_{int} = 0.0508, R_{sigma} = 0.0441]	36110 [R_{int} = 0.0640, R_{sigma} = 0.0497]	16687 [R_{int} = 0.0696, R_{sigma} = 0.0499]	16236 [R_{int} = 0.0752, R_{sigma} = 0.0609]
Data/restraints/parameters	23959/142/1179	36110/46/1669	16687/875/1381	16236/1089/1384
Goodness-of-fit on F^2	1.048	1.041	1.326	1.258
Final R indexes [I>=2σ (I)]	R_1 = 0.0938, wR_2 = 0.2701	R_1 = 0.0996, wR_2 = 0.2932	R_1 = 0.1498, wR_2 = 0.3900	R_1 = 0.1490, wR_2 = 0.3708
Final R indexes [all data]	R_1 = 0.1003, wR_2 = 0.2749	R_1 = 0.1106, wR_2 = 0.3023	R_1 = 0.1938, wR_2 = 0.4230	R_1 = 0.1991, wR_2 = 0.4088
Largest diff. peak/hole / e Å^{-3}	0.46/-0.38	1.16/-0.56	0.46/-0.34	0.48/-0.46

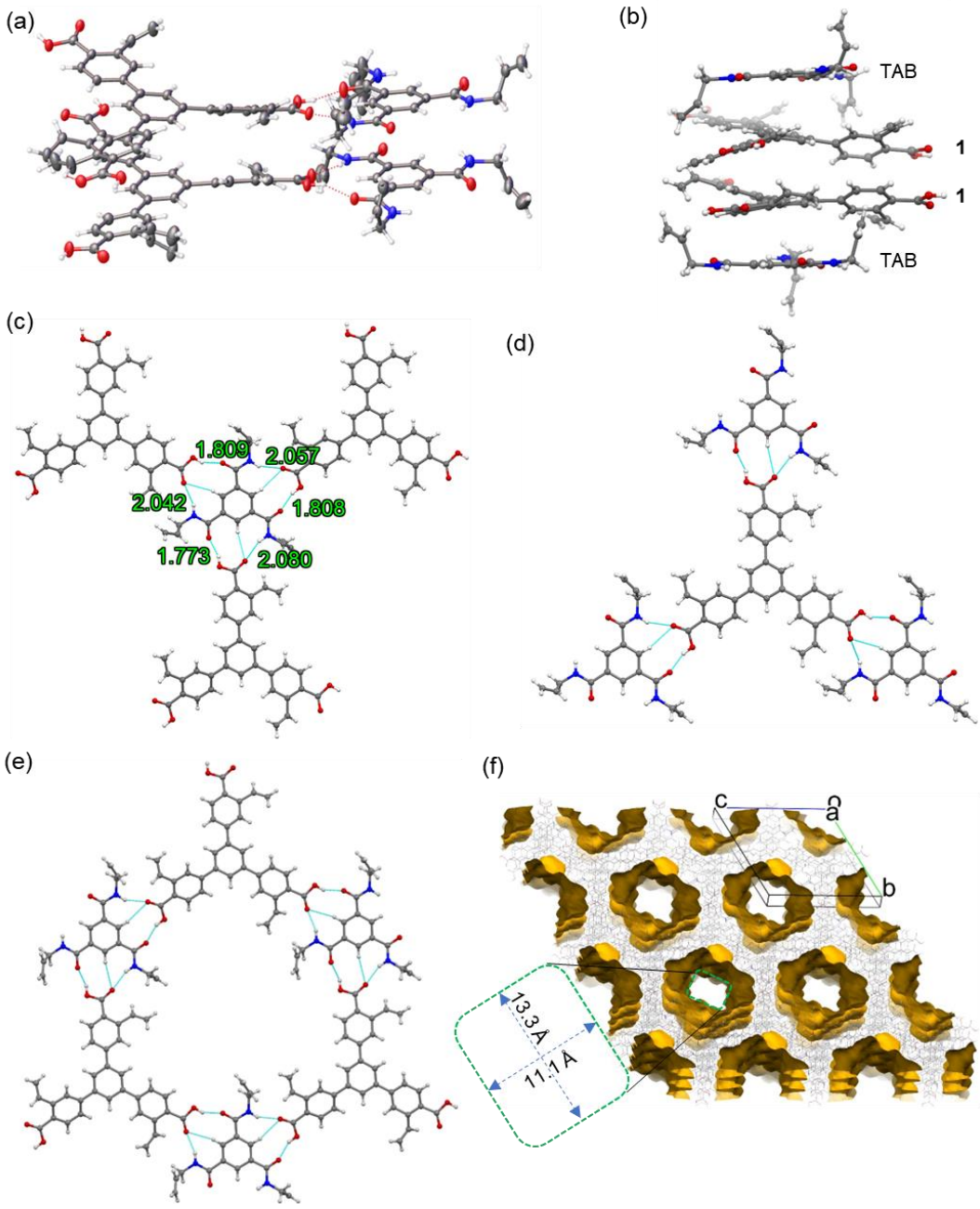

Figure S28. SCXRD analysis of **1**•TAB. (a) The asymmetric unit of **1**•TAB, which contains two of **1** and two-TAB molecules. Molecules are shown in thermal ellipsoids with a 50% probability level. One vinyl group in one of the **1** and one vinyl group in one of the TAB were disordered over two places. (b) ABBA stacking of **1** and TAB units. Hydrogen bonding networks in the crystal lattice showing, (c) one TAB connected with three of **1** and (d) one **1** connected with three TAB. (e) Hexagonal pore formation with a (f) pore aperture of 13.3 Å (length) and 11.1 Å (width) and packing structure of **1**•TAB shown along the a-axis. The packing structure shows the lattice contains a 1-D porous channel along the a-axis. The lattice contains 32%voids (probe radius 1.2Å, grid spacing 0.7Å).

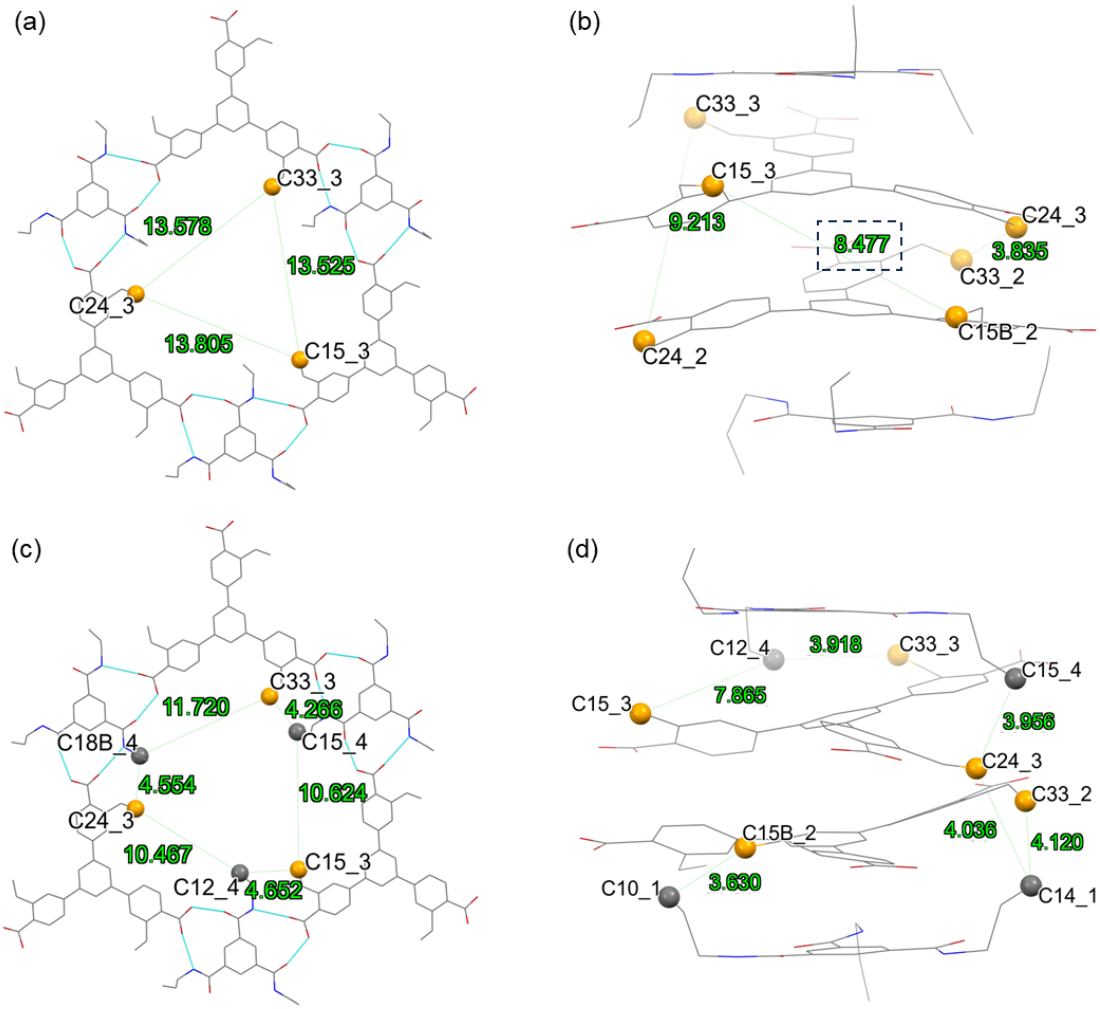

Figure S29. Distances between reactive groups in **1**•TAB. Distances from terminal vinyl carbon of the styrene to terminal vinyl carbon of another styrene group present in the (a) intralayer and (b) interlayer crystal lattice. Distances from terminal vinyl carbon of the styrene to terminal vinyl carbon of allyl groups present in the (c) intralayer and (d) interlayer crystal lattice.

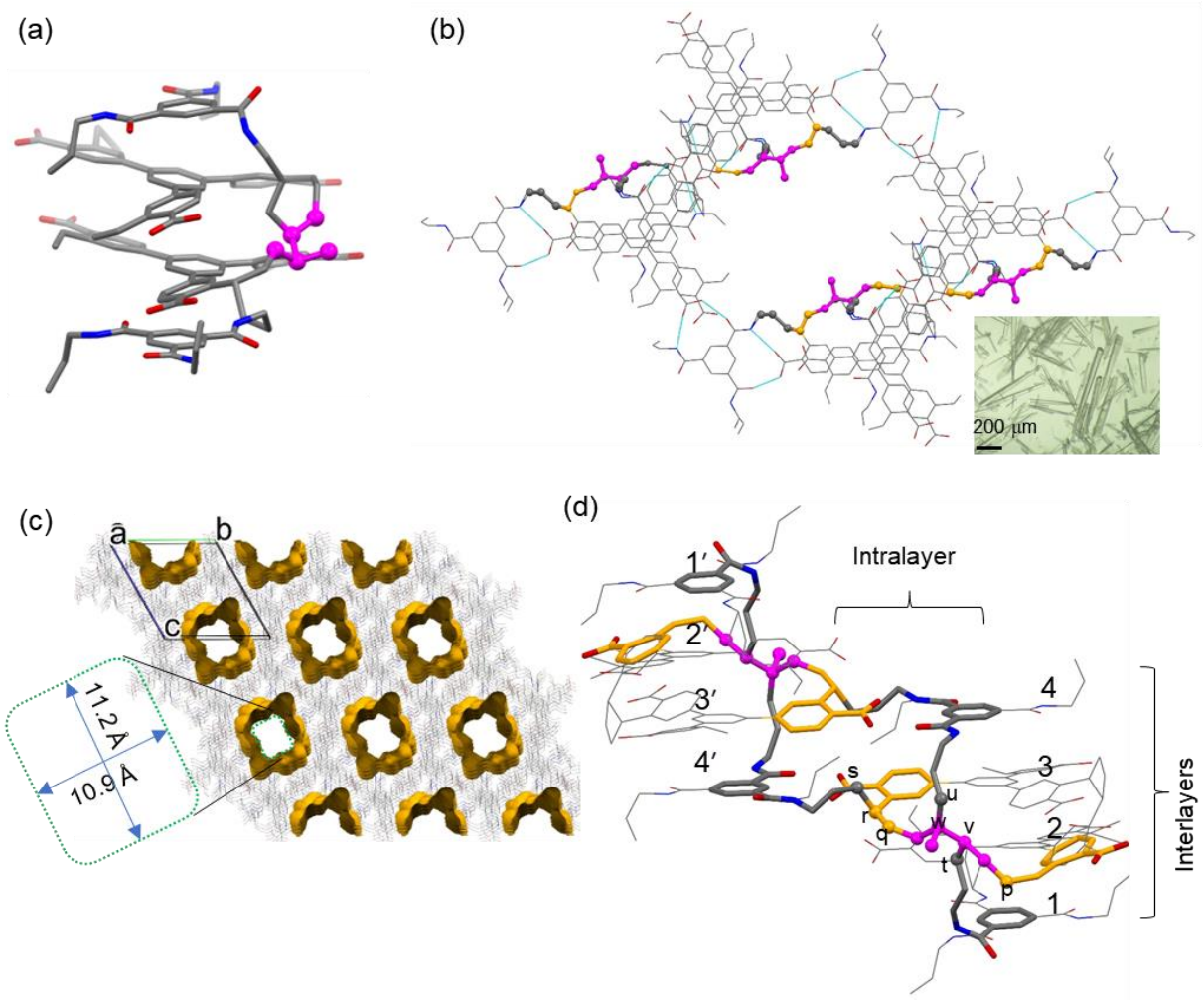

Figure S30. SCXRD analysis of H_COF-107. (a) The asymmetric unit of H_COF contains two **1**, two TAB molecules, and one isoprene (the disordered parts are removed for clarity). Isoprene is shown in the ball and stick model (magenta), and the rest of the molecules are shown in the capped sticks model. (b) The grown hexagonal structure of the H_COF-107 shows the isoprene crosslinker (magenta) in the crystal lattice. (c) The packing diagram of H_COF-107 is shown along the a-axis. The packing structure shows that the lattice contains a 1-D porous channel along the a-axis. The pore aperture is 11.20 Å (length) and 10.9 Å (width) and the lattice contains 26% voids (probe radius 1.2Å, grid spacing 0.7Å). (d) The crosslinking connections between the layers. Crosslinked styrene units are shown in orange, crosslinked TAB units are shown in dark grey, and isoprene is shown in magenta color.

Table S3. Comparison of Iodine value with SCXRD analysis.

Sample	Molecular weight per asymmetric unit	Number of double bonds per asymmetric unit from Iodine value	Number of double bonds per asymmetric unit from SCXRD
1•TAB	1687.86 (Figure S31a)	12.044	12.0
H_COF-107	1760.0 (Figure S31b)	6.11	6.0

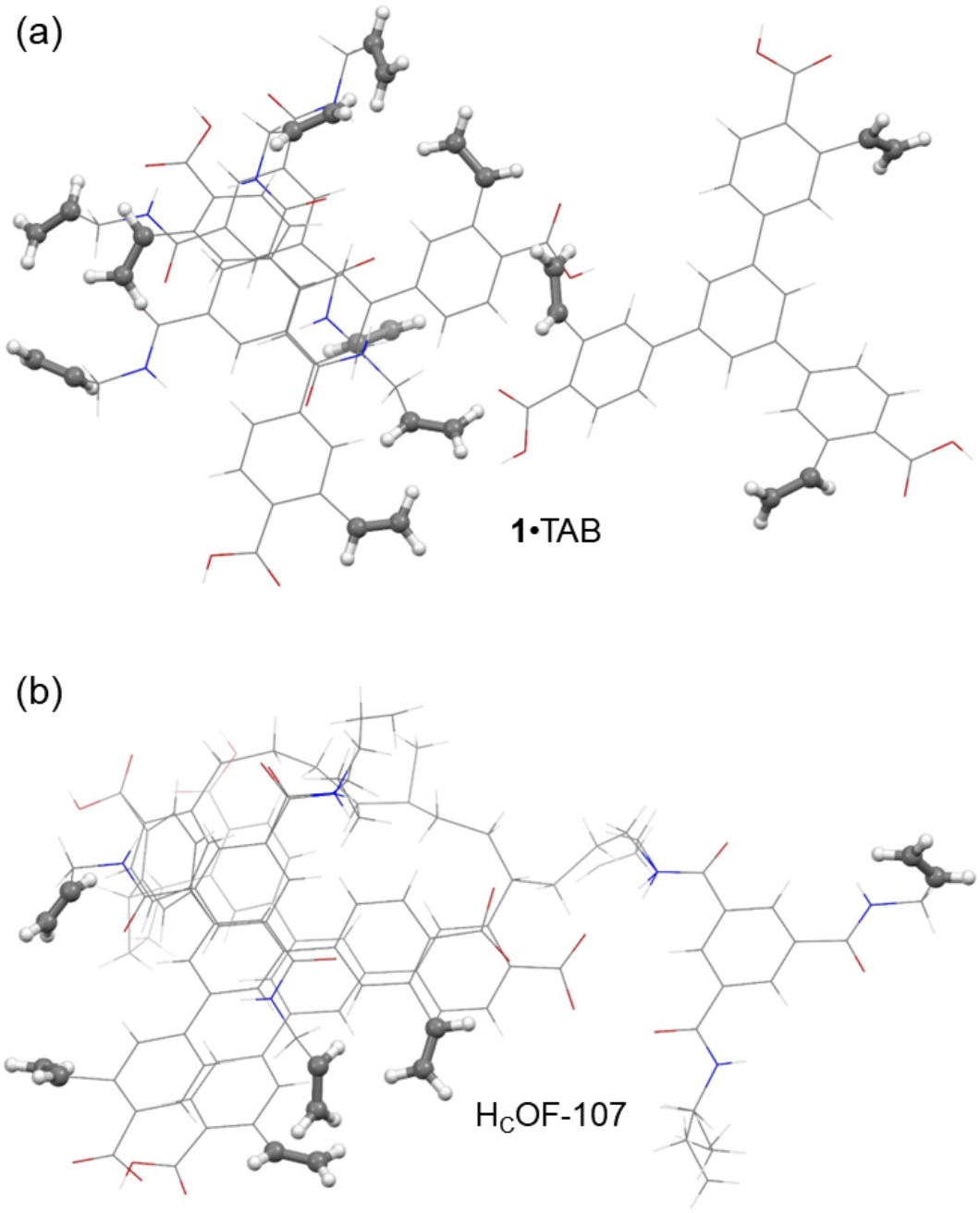

Figure S31: The free olefinic units present per asymmetric unit in (a) **1**•TAB and (b) H_COF-107.

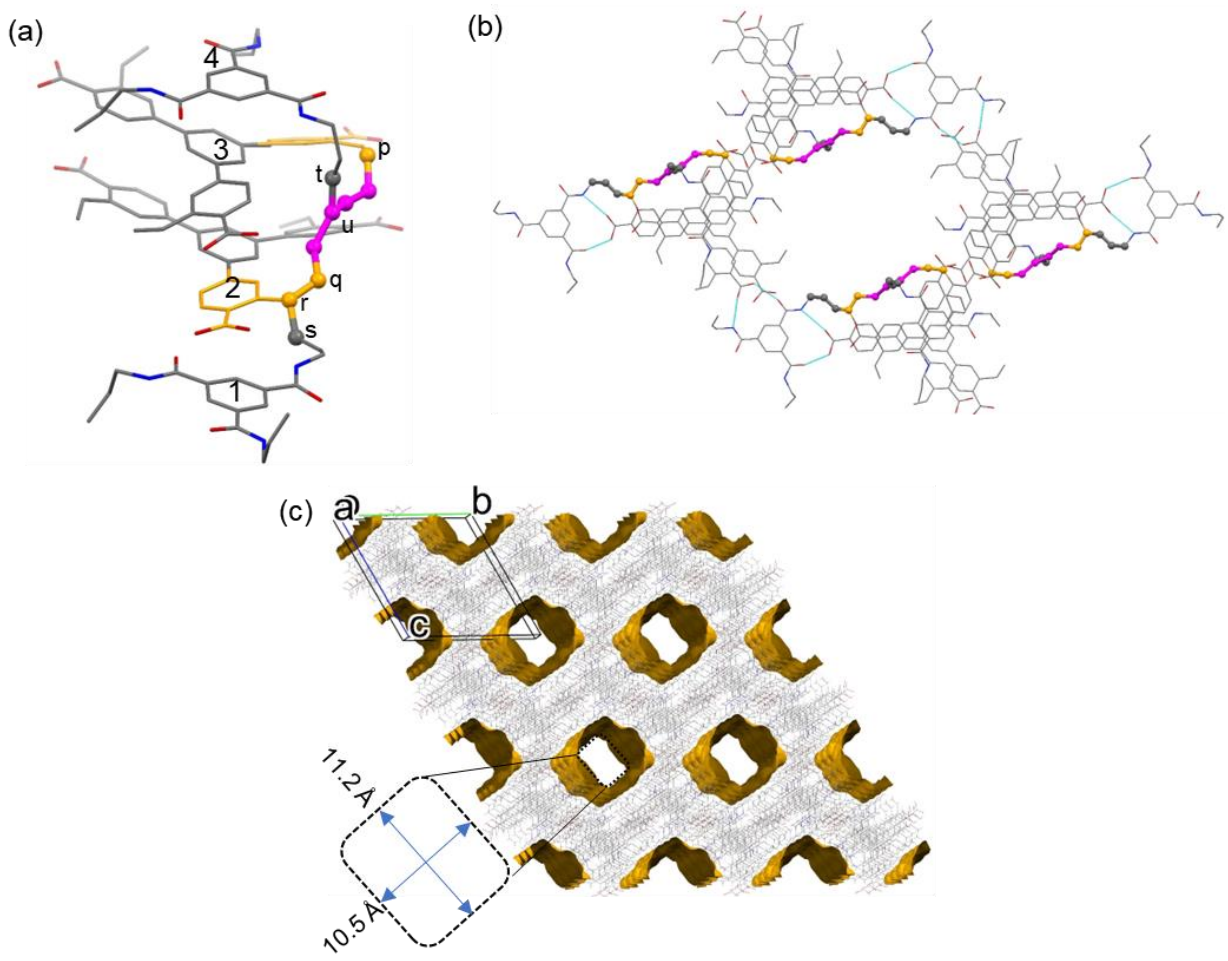

Figure S32. SCXRD analysis of H_COF-106. (a) The asymmetric unit of H_COF-106 contains two **1**, two TAB molecules, and one butadiene (the disordered parts are removed for clarity). Butadiene is shown in the ball and stick model (magenta), and the rest of the molecules are shown either in the capped sticks or in the wireframe model. Crosslinked styrene units are shown in orange, and crosslinked TAB units are shown in dark grey. (b) The grown hexagonal structure of the H_COF-106 shows the isoprene crosslinker (magenta) in the crystal lattice. (c) The packing diagram of H_COF-106 is shown along the a-axis. The pore aperture is 11.2 Å (length) and 10.5 Å (width). The packing structure shows the lattice contains a 1-D porous channel along the a-axis. The lattice contains 23% voids (probe radius 1.2Å, grid spacing 0.7Å).

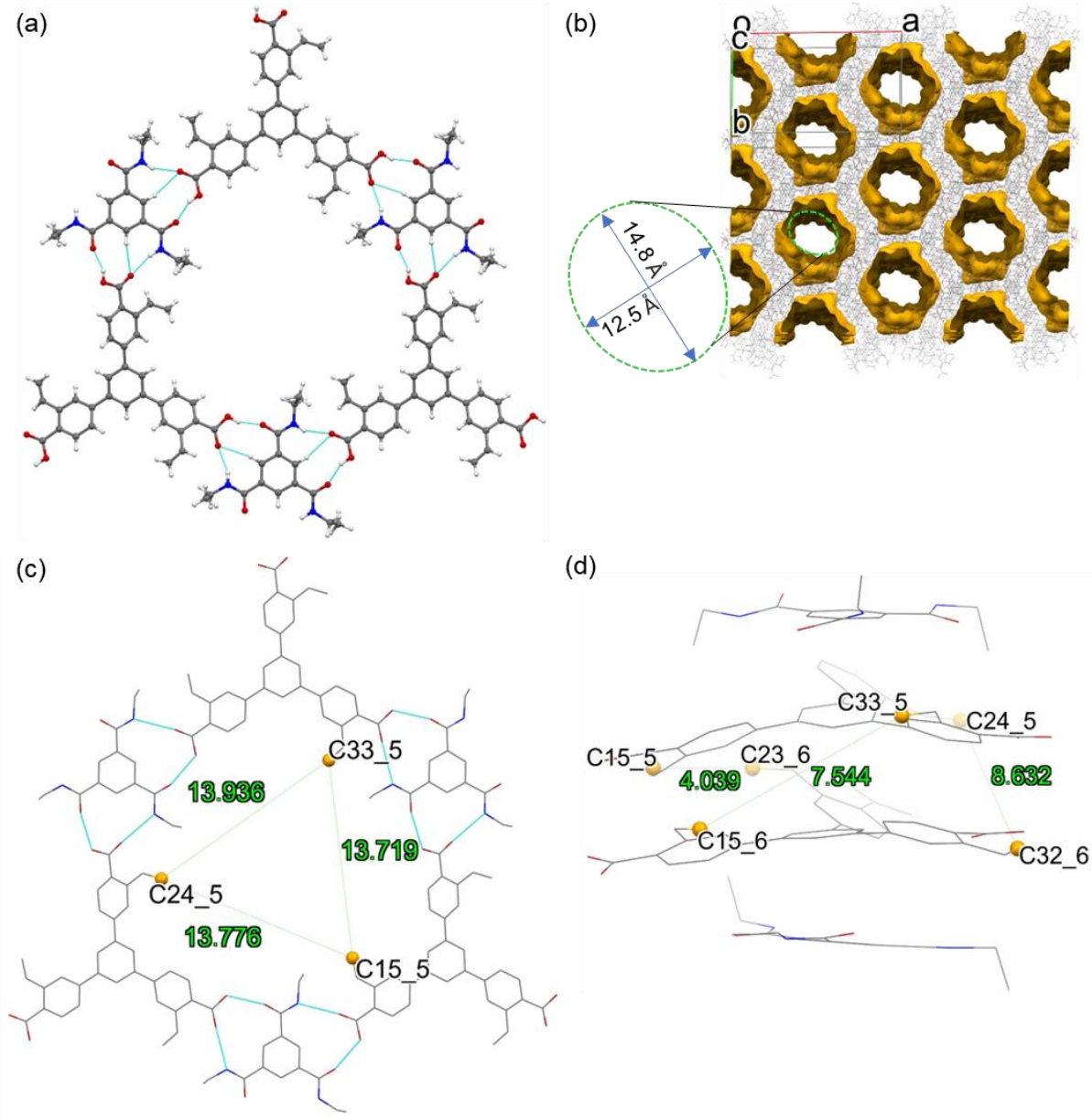

Figure S33. SCXRD analysis of **1**•TEB. (a) Hexagonal pore formation. (b) The packing structure of **1**•TEB is shown along the c-axis with a pore aperture of 14.8 Å (length) and 12.5 Å (width). The packing structure shows that the lattice contains a 1-D porous channel along the c-axis. The lattice contains 35% voids (probe radius 1.2Å, grid spacing 0.7Å). Distances from the terminal vinyl carbon of the styrene to the terminal vinyl carbon of another styrene group are present in the (c) intralayer and (d) interlayer crystal lattice.

Synthesis of 1•TEB and crosslinking trial with isoprene.

High-quality single crystals of **1**•TEB were obtained by slow diffusion of hexane into a 1,4-dioxane solution of **1** and TEB (1.0 *equiv*. to **1**) at room temperature for 7 days. Mother liquor of **1**•TEB was removed, and the crystals were washed three times using hexane (5 mL × 3) and dried under vacuum. **1**•TEB crystals (10 mg) in a 20 mL glass vial were charged with isoprene (2 mL) and 2,2-dimethoxy-2-phenylacetophenone (radical initiator, 0.04 mol %). The vial was kept in the dark for 24 h before being irradiated under UV light (medium-pressure 175-watt Hg lamp) for 72 h with forced air cooling. The crystal samples were collected and washed with an excess of hexane to remove the unreacted isoprene and then dried under a vacuum. Next, the crystal samples were immersed in DMSO-d_6 and heated to boiling for 2-3 min. The residual solution was subjected to ^{1}H NMR analysis. Under the microscope, we observed the crystals dissolve in hot DMSO.

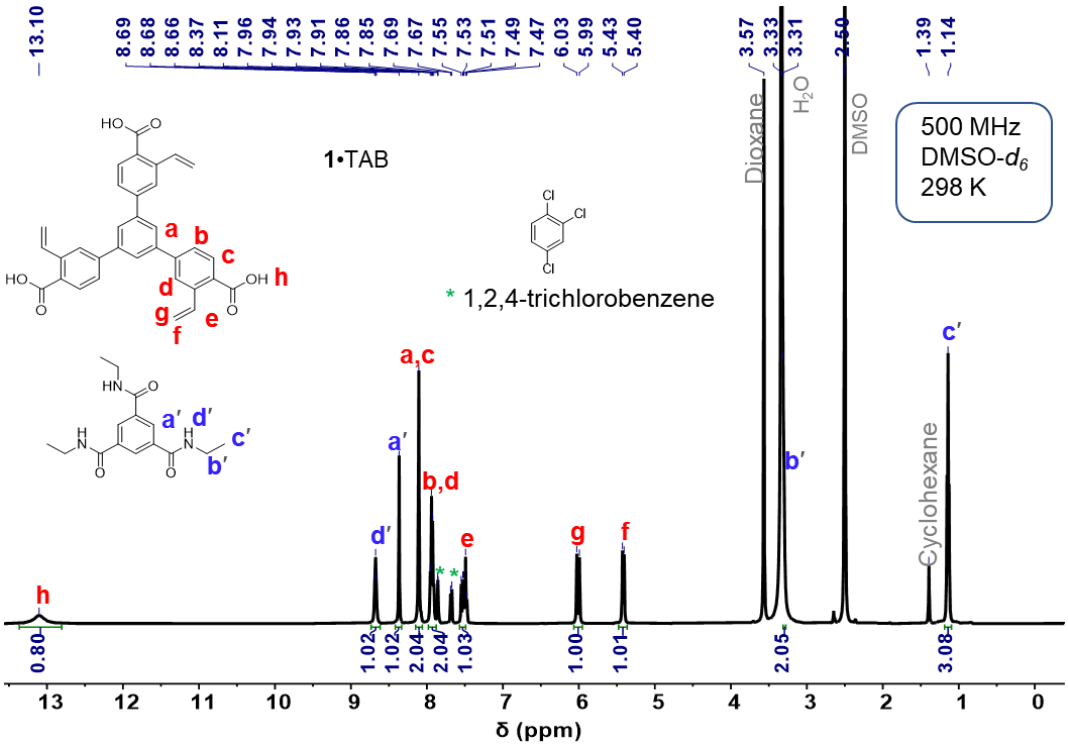

Figure S34. ^{1}H NMR spectrum of **1**•TEB crystals in DMSO-d_6 at 298 K.

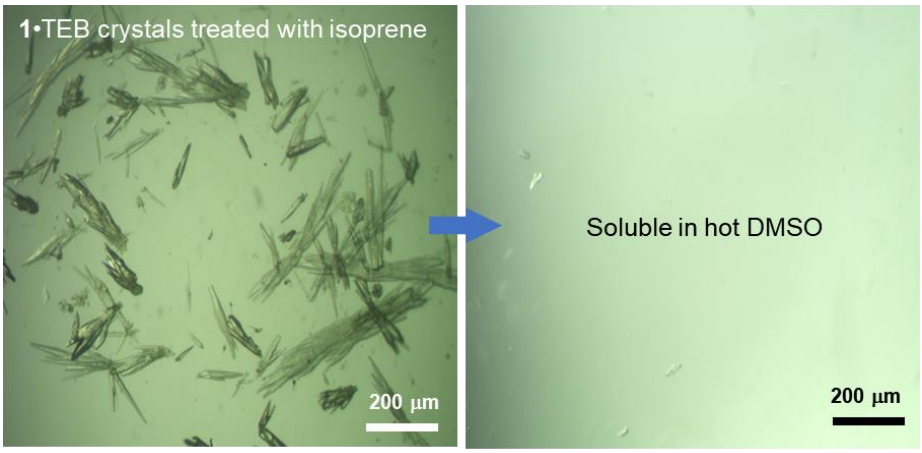

Figure S35. Microscope images of **1**•TEB crystals after crosslinking with isoprene and treatment with boiling DMSO. A Majority of the crystals dissolved in DMSO.

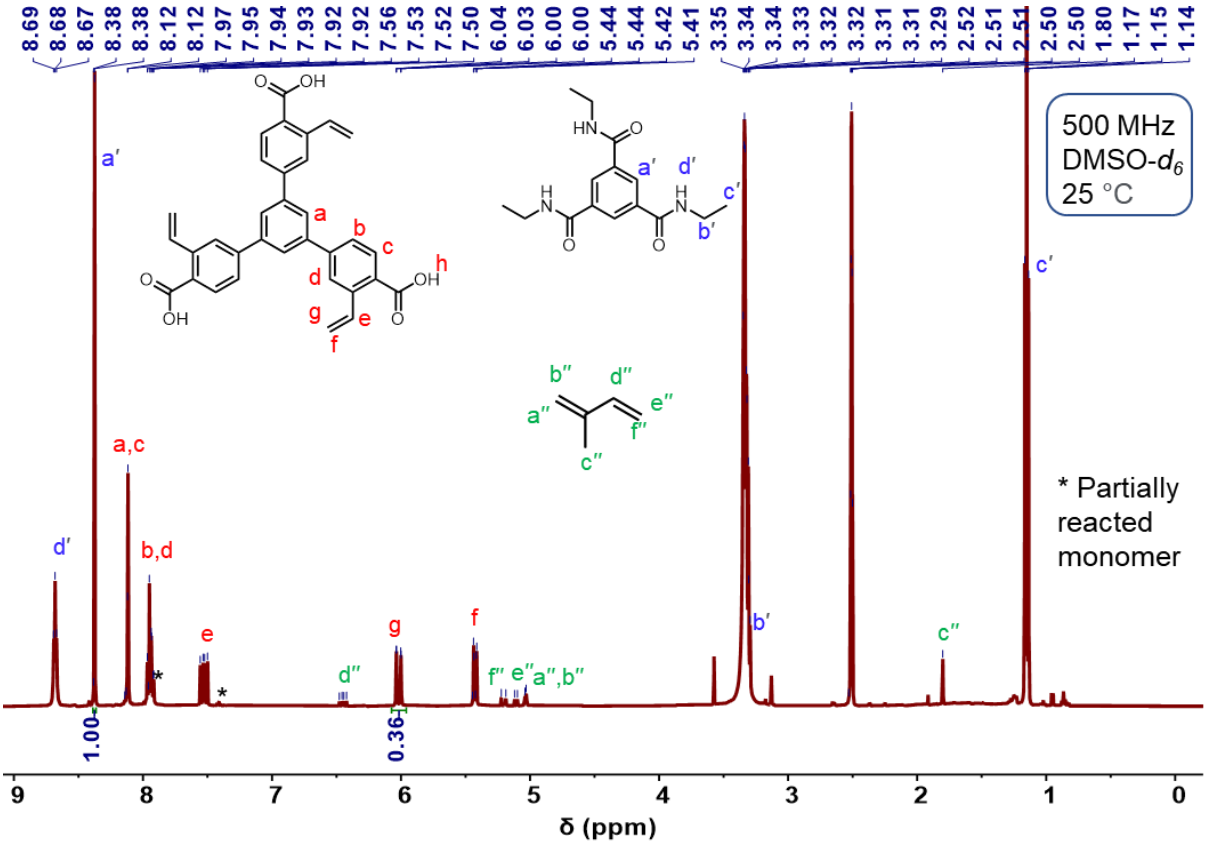

Figure S36. ^{1}H NMR spectrum of isoprene-treated **1**•TEB crystals in DMSO-d_6 at 298 K after crosslinking.

S5. Synthesis and Characterization of H_COF-108

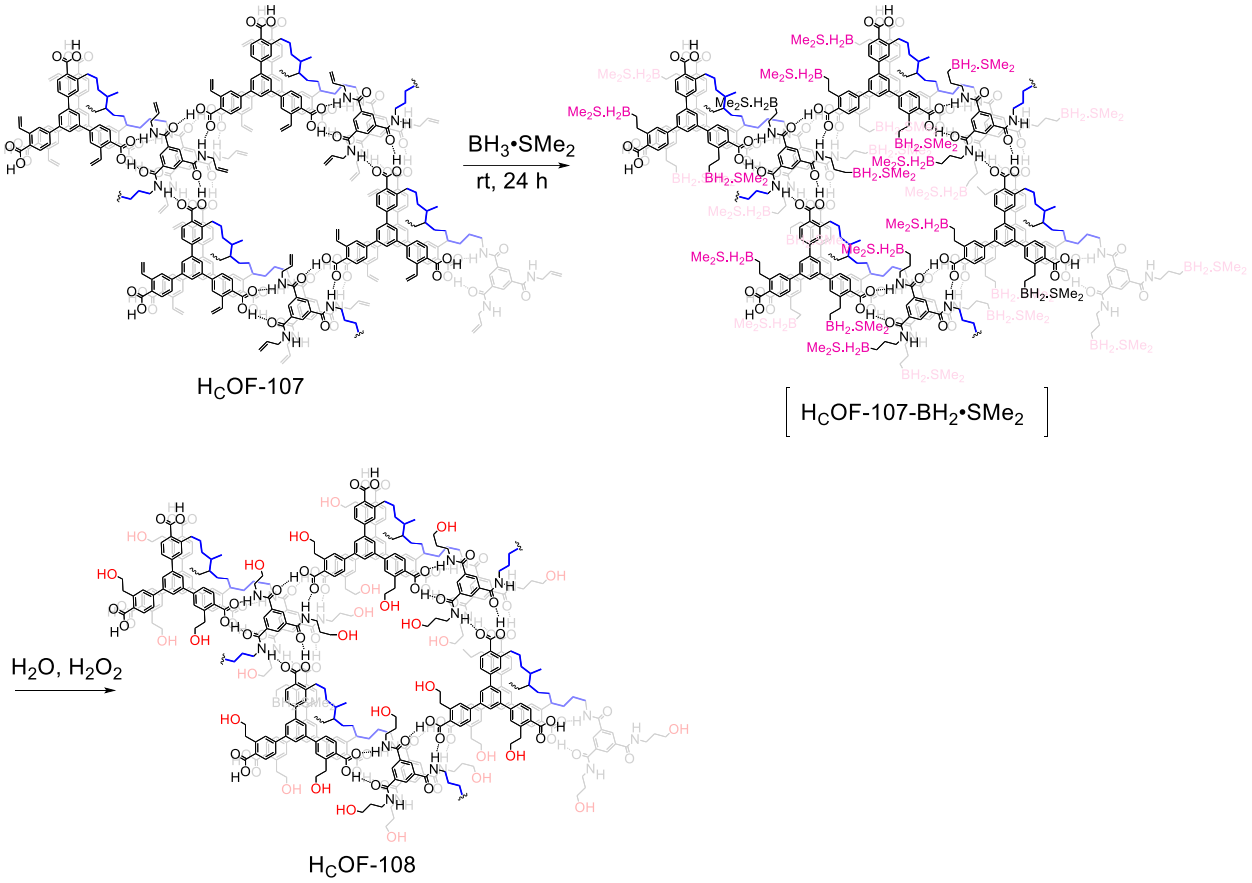

Scheme S6. Synthetic scheme of H_COF-108.

Synthesis of [H_COF-107-BH_2•SMe_2]. H_COF-107 (350 mg) in a 20 mL vial was charged with 5 mL BH_3.SMe_2 (90% BH_3 in dimethyl sulfide) under nitrogen atmosphere. The reaction was stirred for 24 h at room temperature. The material color changed from white to pink color over time. The excess BH_2•SMe_2 was removed under vacuum to obtain H_COF-107-BH_2•SMe_2 (418 mg).

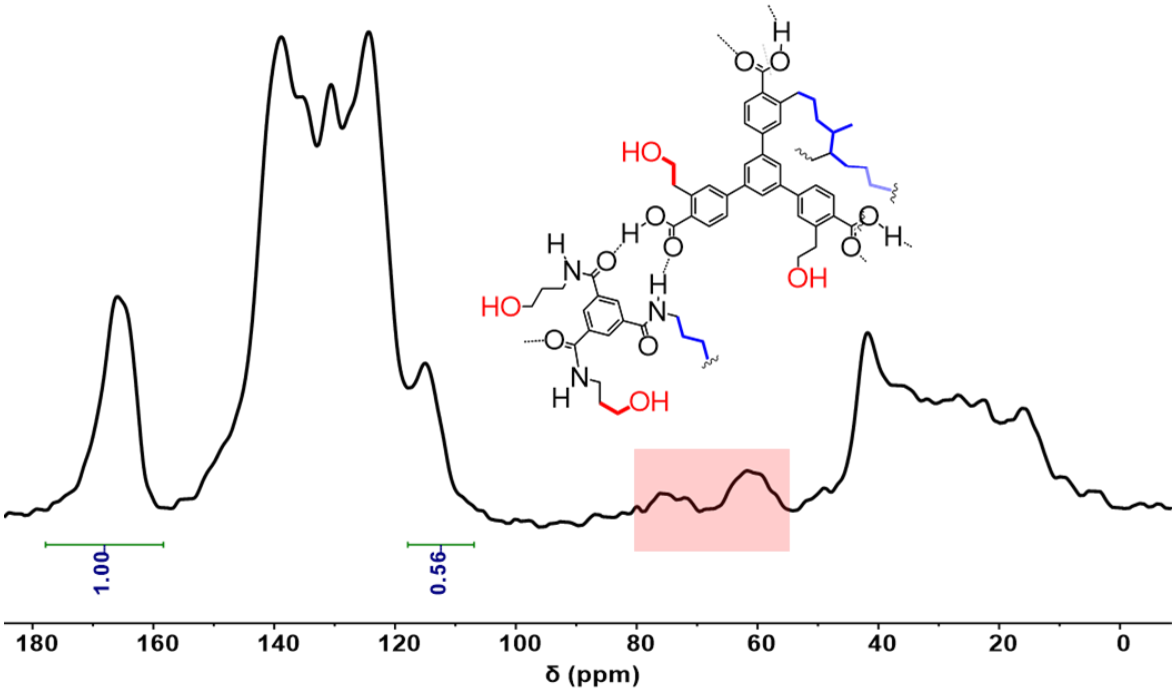

Figure S37. ^{13}C solid-state NMR spectra of H_COF-108.

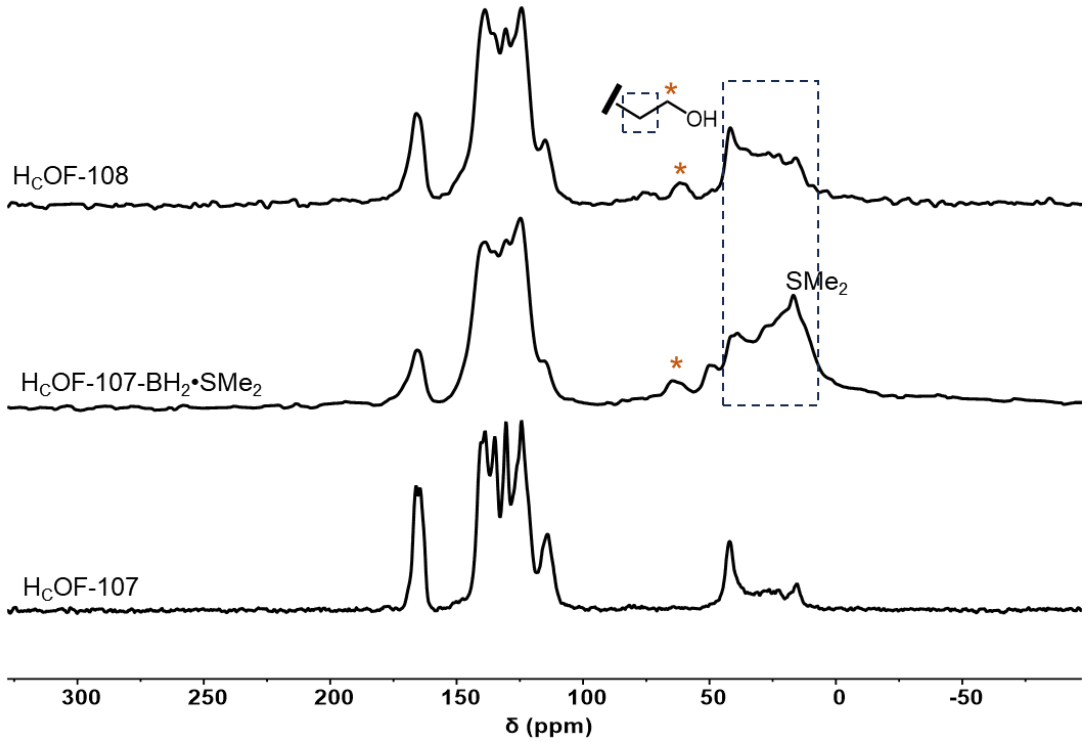

Figure S38. ^{13}C solid-state NMR spectra of H_COF-107, H_COF-107-BH_2•SMe_2, and H_COF-108.

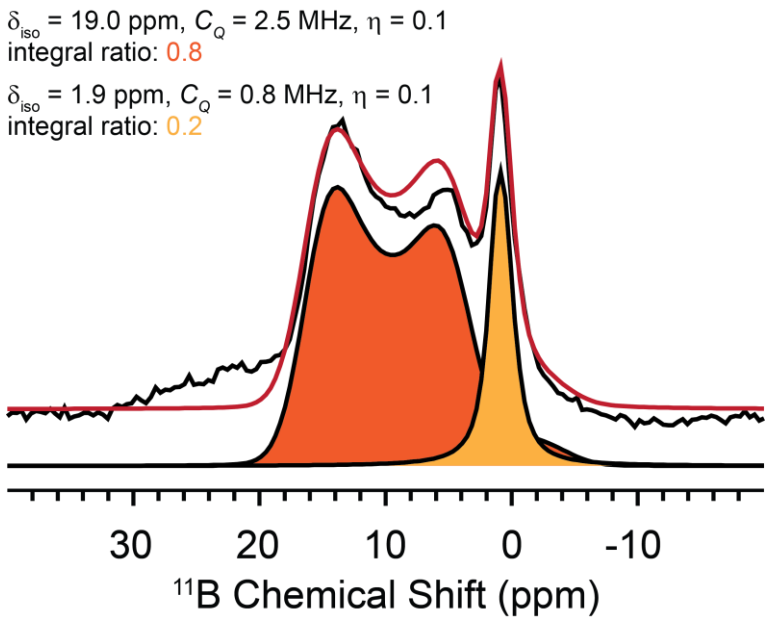

Figure S39. Solid-state ^{11}B NMR of HCOF-107-BH_2•SMe_2. The ^{11}B NMR spectrum was simulated to fit two sites. The higher frequency broad signal is assigned to 3-coordinated ^{11}B sites from boronic acid B.[11] The lower frequency sharp signal is assigned to 4-coordinated ^{11}B sites arising from hydrolyzed borane species like $RB(OH)_3^-$ or $B(OH)_4^-$.

Table S4. Experimental solid-state NMR parameters. (^{1}H spin-lock RF fields, X spin-lock RF fields, CP contact times, recycle delays, number of scans, and MAS Frequency)

Figure	Sample name	Expt.	MAS Frequency (kHz)	CP Contact time (μs)	Recycle delay (s)	Number of scans	Total Expt. Time (h, min)
2, S16	**1**•TAB	^{1}H→^{13}C CP	25	2000	2.4	25600	17 h 30 min
2, S17	H_COF-106	^{1}H→^{13}C CP	25	2000	1.5	69632	29 h 34 min
2, S18	H_COF-107	^{1}H→^{13}C CP	25	2000	2.3	32768	21 h 44 min
2, S37	H_COF-108	^{1}H→^{13}C CP	25	2000	1.8	24576	12 h 26 min
S38	H_COF-107-BH_3•SMe_2	^{1}H→^{13}C CP	25	2000	3.1	20480	17 h 59 min
S39	H_COF-107-BH_3•SMe_2	^{11}B spin echo	25	-	1.0	128	2 min

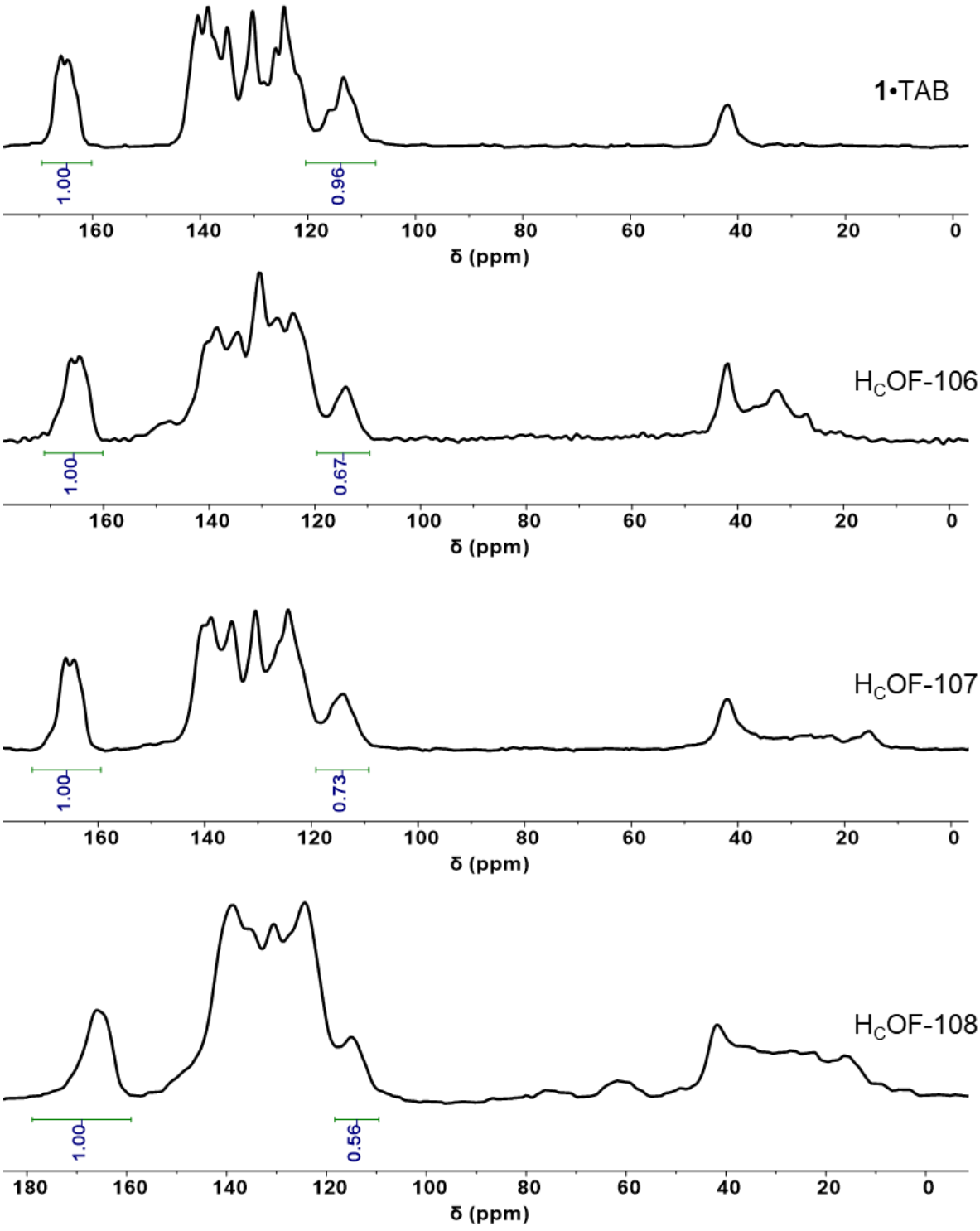

Figure S40. ^{13}C solid-state NMR spectra of **1**•TAB, H_COF-106, H_COF-107, and H_COF-108; showing the integration values of the residual allyl carbons to the carbonyl carbons.

Table S5. Comparison of the integration values (from solid-state NMR) between the carbonyl carbons and allyl carbons.

Figure	Sample name	Carbonyl carbons	Allyl carbons
2, S40	**1**•TAB	1.00	0.96
2, S40	H_COF-106	1.00	0.67
2, S40	H_COF-107	1.00	0.73
2, S40	H_COF-108	1.00	0.56

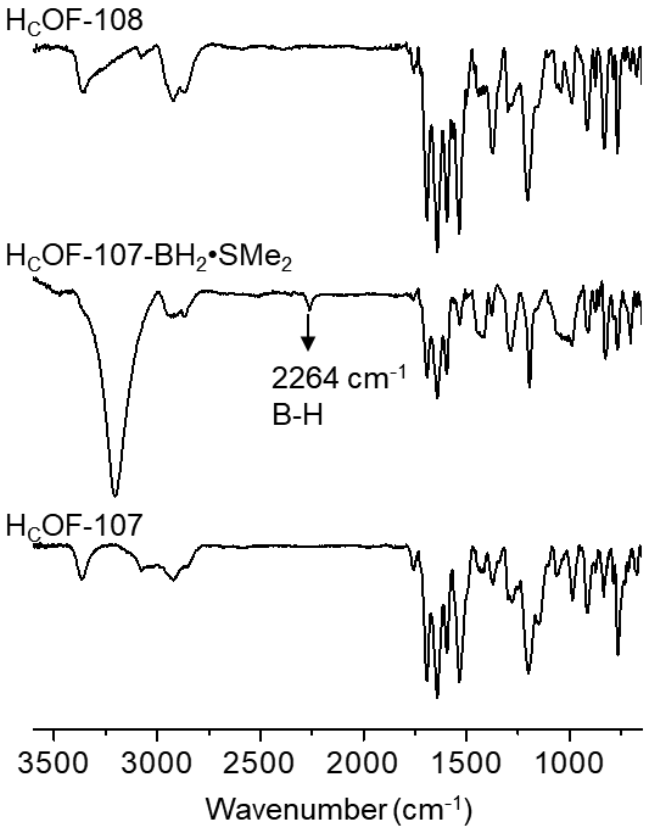

Figure S41. Comparison of IR spectra of H_COF-107, H_COF-107-BH_2•SMe_2, and H_COF-108.

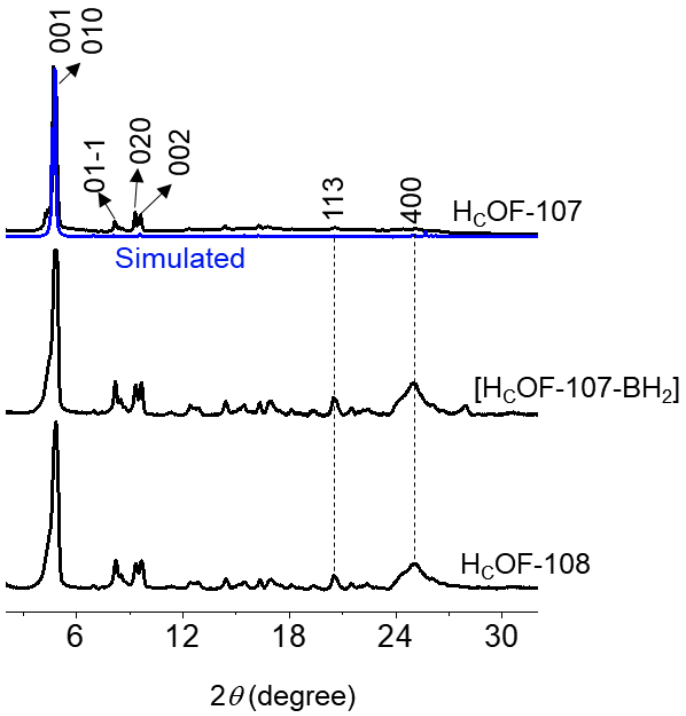

Figure S42. Comparison of simulated and experimental PXRD patterns of H_COF-107, H_COF-107-BH_2•SMe_2, and H_COF-108.

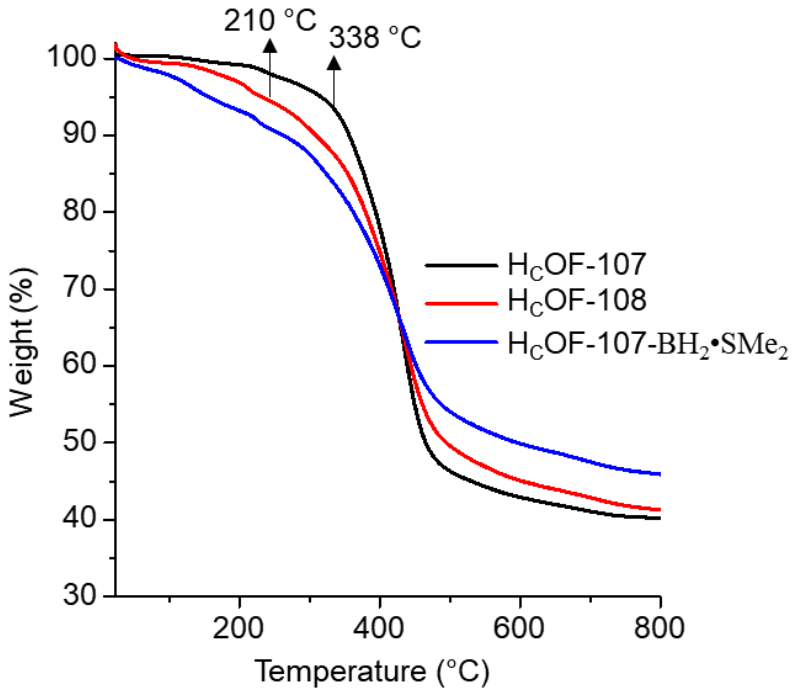

Figure S43. Comparison of TGA profiles of H_COF-107, H_COF-107-BH_2•SMe_2, and H_COF-108.

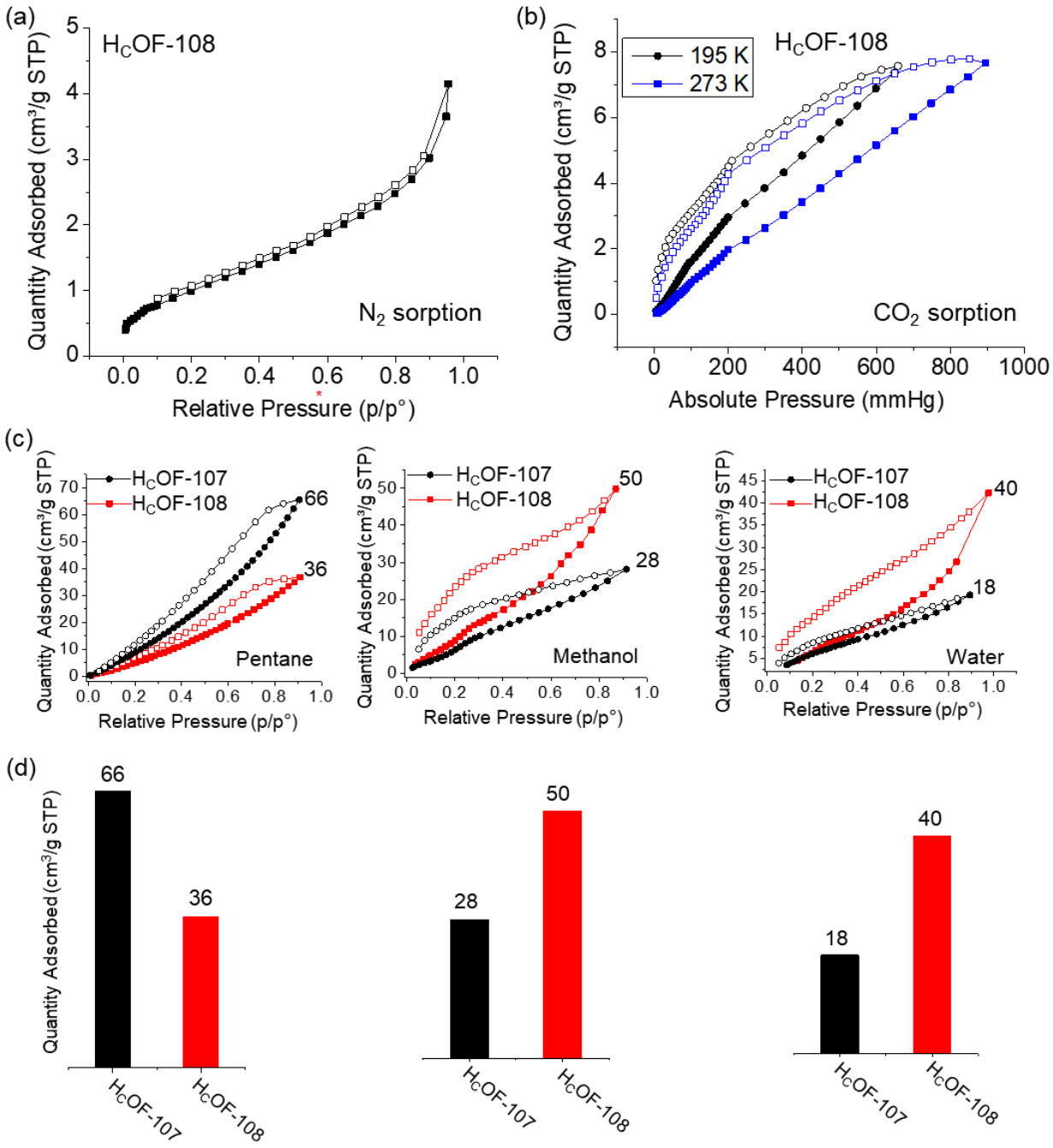

Figure S44. (a) N_2 and (b) CO_2 gas sorption of H_COF-108. (c) and (d) comparison of solvent vapor sorption isotherms of H_COF-107 (black) and H_COF-108 (red).

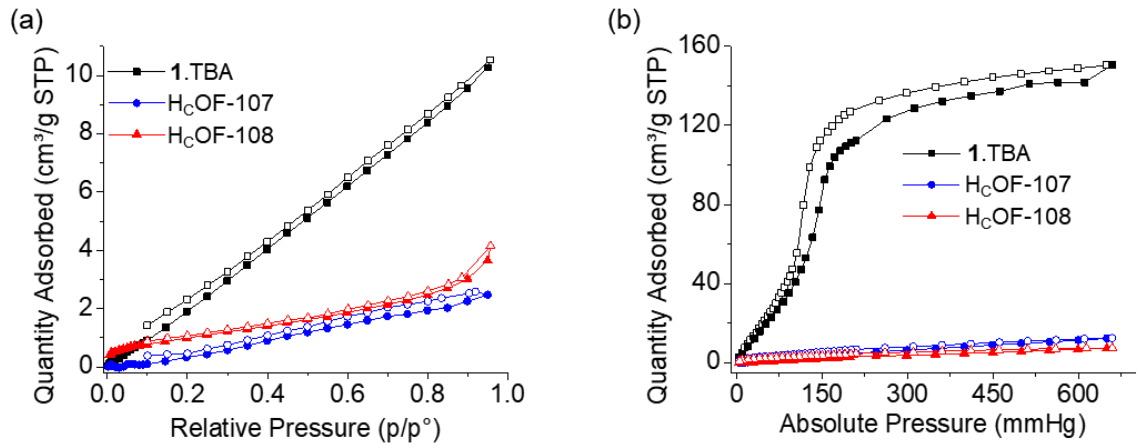

Figure S45. (a) N_2 and (b) CO_2 gas sorption comparison among **1**•TAB (black), H_COF-107 (blue), and H_COF-108 (red).

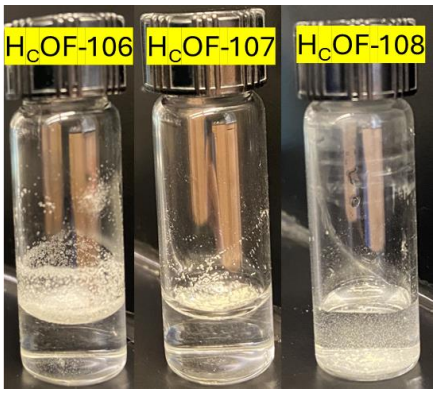

Figure S46. Water miscibility test for H_COF-106, H_COF-107, and H_COF-108. For each test, 5 mg of the respective H_COF was added to 1 mL of water and shaken vigorously. H_COF-106 and H_COF-107, due to their non-polar nature, float on the surface of the water, while the relatively polar H_COF-108 showed better contact with water and suspended in the mixture.

References:

[1] R. K. Harris, E. D. Becker, S. M. C. de Menezes, R. Goodfellow and P. Granger, *Solid State Nucl. Magn. Reson.*, 2002, **22**, 458–483.
[2] A. Pines, M. G. Gibby and J. S. Waugh, *J. Chem. Phys.*, 1972, **56**, 1776–1777.
[3] G. Metz, X. L. Wu and S. O. Smith, *J. Magn. Reson., Ser. A*, 1994, **110**, 219–227.
[4] B. M. Fung, A. K. Khitrin and K. Ermolaev, *J. Magn. Reson.*, 2000, **142**, 97–101.
[5] H. Wu, L. Zhang, Y. Xu, Z. Ma, Z. Shen, X. Fan and Q. Zhou, *J. Polym. Sci. Part A: Polym. Chem.*, 2012, **50**, 1792–1800.
[6] J. W. McCutcheon, *Ind. Eng. Chem. Anal. Ed.*, 1940, **12**, 465–465.
[7] CrysAlisPro 1.171.40.60a (Rigaku Oxford Diffraction, 2019).
[8] G. M. Sheldrick, *Acta Cryst.,* 2015, **A71**, 3-8.
[9] G. M. Sheldrick, *Acta Cryst.,* 2015, **C71**, 3-8
[10] O. V. Dolomanov, L. J. Bourhis, R. J. Gildea, J. A. K. Howard, H. Puschmann, *J. Appl. Cryst.,* 2009, **42**, 339-341.
[11] R. W. Dorn, M. C. Cendejas, K. Chen, I. Hung, N. R. Altvater, W. P. McDermott, Z. Gan, I. Hermans and A. J. Rossini, *ACS Catal.*, 2020, **10**, 13852–13866.